



Published in final edited form as:

Nature. 2019 April ; 568(7751): 249–253. doi:10.1038/s41586-019-1041-6.

## A NIK-SIX signaling axis controls inflammation by targeted silencing of noncanonical NF- $\kappa$ B

Zixu Liu<sup>1</sup>, Katrina B. Mar<sup>1</sup>, Natasha W. Hanners<sup>1</sup>, Sofya S. Perelman<sup>1</sup>, Mohammed Kanchwala<sup>2</sup>, Chao Xing<sup>2,3,4</sup>, John W. Schoggins<sup>1</sup>, Neal M. Alto<sup>1,\*</sup>

<sup>1</sup>Department of Microbiology, University of Texas Southwestern Medical Center, 5323 Harry Hines Boulevard, Dallas, Texas, 75390-8816, USA

<sup>2</sup>Eugene McDermott Center for Human Growth and Development, University of Texas Southwestern Medical Center, 5323 Harry Hines Boulevard, Dallas, Texas, 75390-8816, USA

<sup>3</sup>Department of Bioinformatics, University of Texas Southwestern Medical Center, 5323 Harry Hines Boulevard, Dallas, Texas, 75390-8816, USA

<sup>4</sup>Department of Population and Data Sciences, University of Texas Southwestern Medical Center, 5323 Harry Hines Boulevard, Dallas, Texas, 75390-8816, USA

### SUMMARY

The non-canonical NF- $\kappa$ B signaling cascade is essential for lymphoid organogenesis, B-cell maturation, osteoclast differentiation, and inflammation in mammals<sup>1,2</sup>, whereas dysfunction of this system is associated with human diseases, including immunological disorders and cancer<sup>3–6</sup>. While controlled expression of NF- $\kappa$ B Inducing Kinase (NIK) is the rate-limiting step in non-canonical NF- $\kappa$ B activation<sup>2,7</sup>, mechanisms of inhibition remain largely unknown. Here, we report the identification of the *sine oculis* homeobox homolog family transcription factors SIX1 and SIX2 as essential inhibitory components of the non-canonical NF- $\kappa$ B signaling pathway. The developmentally silenced *SIX*-proteins are reactivated in differentiated macrophages by NIK-mediated suppression of the ubiquitin proteasome pathway. Consequently, SIX1 and SIX2 target a subset of inflammatory gene promoters and directly inhibit RelA and RelB *trans*-activation function in a negative feedback circuit. In support of a physiologically pivotal role for *SIX*-proteins in host immunity, human SIX1 transgene suppressed inflammation and promoted the recovery of mice from endotoxic shock. In addition, SIX1 and SIX2 protected RAS/p53-driven lung adenocarcinoma cells from inflammatory cell death induced by SMAC-mimetic chemotherapeutic agents, small-molecule activators of the non-canonical NF- $\kappa$ B pathway.

**Reprints and permissions information** is available at [www.nature.com/reprints](http://www.nature.com/reprints). Users may view, print, copy, and download text and data-mine the content in such documents, for the purposes of academic research, subject always to the full Conditions of use: [http://www.nature.com/authors/editorial\\_policies/license.html#terms](http://www.nature.com/authors/editorial_policies/license.html#terms)

\***Correspondence and requests for materials** should be addressed to N.M.A. [neal.alto@utsouthwestern.edu](mailto:neal.alto@utsouthwestern.edu).

#### AUTHOR CONTRIBUTIONS

Z.L. and N.M.A. conceived and designed the study. Unless otherwise specified, Z.L. performed all experiments. K.B.M. assisted in mouse experiments. N.W.H. performed West Nile Virus infection. S.S.P. performed RNA-seq to identify NIK-stimulated genes. M.K. and C.X. performed bioinformatics analysis of RNA-seq data. J.W.S. designed the genetic screening platform for bacteria and viruses and provided critical input into project directions. Z.L. and N.M.A. analyzed data and wrote the manuscript with editorial input from all authors.

#### COMPETING INTERESTS

The authors declare no competing interests.

Collectively, our study reveals a NIK-*SIX* signaling axis that fine-tunes inflammatory gene expression programs under both physiological and pathological conditions.

Our investigation into mechanisms of cell-autonomous immunity revealed that the *sine oculis* (*so*) homeobox gene family members SIX1 and SIX2 are integral components of the non-canonical NF- $\kappa$ B signaling pathway. Briefly, we found that long term exposure of U-2 OS cells with CD40 ligand (*TNFSF5*)<sup>8</sup> restricted infection by two evolutionarily diverse intracellular pathogens, Gram-positive *Listeria monocytogenes* (*Lm*) and Gram-negative *Shigella flexneri* (*Sf*) (Fig. 1a, b). This cell autonomous immune mechanism was dependent on signaling through the non-canonical NF- $\kappa$ B kinase NIK (*MAP3K14*), but not the canonical NF- $\kappa$ B kinase TAK1 (*MAP3K7*) (Extended Data Fig. 1a–g). In addition, ectopic expression NIK, but not TAK1, potently inhibited bacterial infection (Fig. 1c and Extended Data Fig. 1h–j). Previous studies indicate that NIK also inhibits both positive- and negative-sense single stranded RNA viral infection<sup>9</sup>, suggesting that activation of the non-canonical NF- $\kappa$ B signaling pathway is broadly anti-microbial.

To identify key genetic factors involved in the anti-microbial response to non-canonical NF- $\kappa$ B pathway activation, we generated a cDNA library encompassing 237 genes induced by ectopic expression of NIK (mimicking the anti-microbial conditions in Fig. 1c). The rates of bacterial and viral infection were evaluated in host cells transduced with each of the 237 NIK-stimulated genes in a one-gene to one-well format (Extended Data Fig. 2, Table S1 and S2). A subset of NIK-stimulated genes reproducibly inhibited either bacterial or viral infection, including components of the non-canonical NF- $\kappa$ B signaling pathway (e.g. *CD40*, *MAP3K8*, and *RelB*) as well as anti-viral effectors (e.g. *IRF1*, *OAS2*, and *IFI6*) (Fig. 1d). However, two homologous genes, *SIX1* and *SIX2*, specifically caught our attention because while these genes were activated by NIK, they induced an opposite phenotype to other NIK-stimulated genes by potently enhancing bacterial and viral infection of host cells (Fig. 1d, e).

*SIX1* and *SIX2* are lineage specific transcription factors that define progenitor cell identity in developing organs and are thought to be silenced in adult tissues<sup>10,11</sup>. We sought to determine if endogenous *SIX*-proteins are reactivated in terminally differentiated immune cells under physiological infection conditions. *Lm* infection of primary Bone Marrow Derived Macrophage (BMDMs) stimulated *Six1* transcription (~2 fold) and late phase Six1 protein accumulation (Fig. 2a–c). Interestingly, Six1 protein expression, but not mRNA induction, was potently suppressed in *Lm* infected BMDMs isolated from *Nik*<sup>-/-</sup> mice (*Map3k14* gene knockout; Fig. 2a, c and Extended Data Fig. 3a). *De novo SIX*-protein synthesis was also observed in human fibroblasts stimulated with two distinct non-canonical NF- $\kappa$ B agonists: TWEAK, a TNF-family cytokine that signals through the FN14 receptor<sup>12</sup>, and BV6, a SMAC-mimetic compound that promotes rapid NIK protein accumulation through cIAP1/2 inhibition<sup>13,14</sup> (Fig. 2d, e). Importantly, *NIK*<sup>-/-</sup> fibroblasts failed to express *SIX*-proteins under these conditions. Finally, we found that long-lasting treatment (24 hours) of cells with traditional canonical NF- $\kappa$ B pathway agonists (e.g. TNF and LPS) induced *SIX1* and *SIX2* through a mechanism requiring signaling cross talk with NIK<sup>15</sup> (Extended Data Fig. 3b–e). These data indicate that NIK induces *SIX*-proteins expression under a variety of inflammatory conditions.

We noted that recombinant SIX1 and SIX2 proteins were expressed at unusually low levels when driven by a strong Cytomegalovirus (CMV) promoter (Extended Data Fig. 3f, g). Co-transfection of NIK or long-lasting treatment of cells with non-canonical NF- $\kappa$ B agonists induced CMV-driven *SIX*-proteins expression revealing a post-transcriptional mechanism of control (Extended Data Fig. 3f–h). Application of the 26S proteasome inhibitor MG132 also induced rapid accumulation of CMV-driven *SIX*-proteins in HEK293 cells and endogenous *SIX*-proteins in BMDMs and human fibroblasts suggesting that these proteins are constitutively marked for ubiquitin-mediated degradation<sup>16</sup> (Extended Data Fig. 3i–k). Detailed kinetic analysis of endogenous SIX1 and SIX2 protein expression during non-canonical NF- $\kappa$ B pathway activation (Extended Data Fig. 3l) and investigation into the ubiquitination status of SIX2 (Extended Data Fig. 3m) revealed a concerted mechanism of *SIX*-protein reactivation: 1) induction of *SIX* gene expression through secondary transcription, and 2) *SIX*-protein stabilization through NIK-dependent inhibition of the ubiquitin/proteasome pathway (Extended Data Fig. 3n).

*SIX*-family members regulate gene expression programs in development<sup>17</sup>. However, mutations that prevented assembly of transcriptional co-activator complexes had no bearing on the immunological activity of SIX2 implying an alternative mechanism of action (Extended Data Fig. 4a)<sup>18</sup>. We found that *SIX*-proteins suppressed NIK-mediated immunity suggesting they may negatively regulate non-canonical NF- $\kappa$ B (Extended Data Fig. 4b–f). Whole genome RNA-seq was used to test this hypothesis. Chronic activation of non-canonical NF- $\kappa$ B by ectopic expression of NIK induced transcription of 891 genes, including those with primary and secondary inflammatory response signatures (Extended Data Fig. 4g, h and Table S3). Remarkably, nearly 30% of these genes were potently suppressed by SIX2, including cytokines and chemokines that harbor consensus  $\kappa$ B transcriptional binding sites or that are indirectly stimulated by NF- $\kappa$ B (Extended Data Fig. 4i). Inhibition of *IL-1 $\beta$* , *IL-8*, *IL-13*, *IL-33*, *CCL3*, *CCL19*, *CXCL1*, and *CXCL2* by SIX2 was confirmed by quantitative PCR with reverse transcription (qRT-PCR) (Extended Data Fig. 4j). In addition, *SIX1*<sup>-/-</sup> *SIX2*<sup>-/-</sup> cells exhibited enhanced transcription of these genes after long term cytokine stimulation (Fig. 2f) or viral transduction of NIK (Fig. 2g), indicating that endogenous *SIX*-proteins negatively regulate inflammatory gene expression programs.

A subset of the *SIX* regulated genes were induced by the canonical NF- $\kappa$ B subunit RelA (e.g. *IL-1 $\beta$*  and *IL-8*) and others required non-canonical RelB (e.g. *IL-13*, *IL-33*, *CCL3*, *CCL19*, *CXCL1*, and *CXCL2*)<sup>2</sup> (Extended Data Fig. 5a–c). To then determine if *SIX*-proteins inhibit multiple NF- $\kappa$ B isoforms as these data suggest, we analyzed luciferase reporter expression driven by 5 $\times$  $\kappa$ B binding sites. Transient transfection of *SIX*-family members inhibited 5 $\times$  $\kappa$ B-*LUC* stimulated by long term cellular application of canonical and non-canonical NF- $\kappa$ B agonists TNF and LT $\alpha$ 1 $\beta$ 2, respectively (Extended Data Fig. 5d, e). The potency of SIX2 was equivalent to well-known inhibitors of NF- $\kappa$ B including I $\kappa$ B super repressor and A20 and was much stronger than both WIP1 and PIAS1 (Extended Data Fig. 5f)<sup>19–22</sup>. Direct studies on *RelA*<sup>-/-</sup> and *RelB*<sup>-/-</sup> cells confirmed that the *SIX*-proteins suppress transcription by both the canonical and non-canonical NF- $\kappa$ B isoforms (Extended Data Fig. 5g). Thus, SIX1 and SIX2 are negative regulatory components of the non-

canonical NF- $\kappa$ B pathway by virtue of their NIK-dependent expression, and not by differential recognition of RelA or RelB target genes.

Mechanistic investigations suggested that *SIX*-proteins exhibit gene proximal inhibitory activities (Extended Data Fig. 6a–c). *SIX1* bound promoter regions neighboring the  $\kappa$ B sequence(s) of the *IL-1 $\beta$* , *IL-8*, and *CCL3* genes indicating it was primed for transcriptional inhibition (Fig. 3a and Extended Data Fig. 6d, e). Cytokine treatment induced further recruitment of *SIX1* to these genes (Fig. 3a and Extended Data Fig. 6d). Importantly, the ability of *SIX1* to occupy inflammatory gene promoters under both quiescent and stimulated conditions explains the observed increase in *IL-1 $\beta$* , *IL-8*, and *CCL3* mRNA expression in *SIX1*<sup>-/-</sup> *SIX2*<sup>-/-</sup> cells (see Fig. 2f).

*SIX*-proteins formed a stable complex with nuclear RelA and RelB (Fig. 3b). Interestingly, this interaction did not affect recruitment of NF- $\kappa$ B to target gene promoters (Extended Data Fig. 6f). In addition, *SIX2* inhibited both GAL4-RelA and GAL4-RelB activation of a 5 $\times$ GAL4 luciferase reporter gene, a reconstituted system that measures NF- $\kappa$ B transcriptional activity independent of its DNA binding preference<sup>23</sup> (Fig. 3c and Extended Data Fig. 6g). These data suggested that *SIX*-proteins inhibit the *trans*-activation function of NF- $\kappa$ B. In support of this conclusion, *SIX2* directly interacted with the *trans*-activation domain of RelA (TAD; residues 473–522), the functional region of NF- $\kappa$ B that recruits chromatin remodeling enzymes and basal transcriptional machinery including RNA Pol II<sup>24</sup> (Fig. 3d). Knockout of *SIX1* and *SIX2* increased RNA Pol II occupancy of *IL-1 $\beta$*  and *IL-8* genes in both basal and cytokine treated fibroblasts (Fig. 3e). Collectively, these data support an inhibitory model by which *SIX*-proteins regulate the *trans*-activation function of NF- $\kappa$ B at inflammatory gene promoters in a negative feedback loop (Extended Data Fig. 6h).

We next sought evidence that *SIX*-proteins suppress inflammatory gene expression programs *in vivo*. Knockout of *Six1* or *Six2* causes embryonic lethality<sup>10</sup>. We therefore adapted a doxycycline inducible system for broad tissue expression of human *SIX1* transgene in adult mice (Extended Data Fig. 7a–d)<sup>25</sup>. Since doxycycline is a powerful antibiotic, we monitored the inflammatory response and progression of disease in mice exposed to bacterial lipopolysaccharide (LPS). *SIX1* suppressed transcription of inflammatory mediators induced by LPS treatment of peritoneal macrophage *ex vivo*, indicating that the human transgene maintains its function across species (Extended Data Fig. 7e). Remarkably, expression of *SIX1* provided nearly complete protection of mice from lethal LPS challenge as compared to littermate controls (Fig. 4a and Extended Data Fig. 7f). While the clinical signs of septic shock were indistinguishable between genotypes six hours post-LPS injection, *SIX1* expressing mice made a near complete recovery over the time course of experiment (Fig. 4b). This recovery correlated with a reduction of inflammatory mediators in serum of *SIX1* expressing mice (Fig. 4c). While these findings clearly indicate that *SIX*-proteins promote inflammatory resolution *in vivo*, we suspect that reactivation of *SIX1* or *SIX2* will have cell-type specific functions under physiological conditions associated with non-canonical NF- $\kappa$ B activation.

We then searched for a second, alternative line of evidence that *SIX*-proteins regulate biological systems associated with non-canonical NF- $\kappa$ B function. Previous studies indicate

that combinatorial application of SMAC-mimetic compounds (e.g. BV6) and TNF promotes cancer cell death, including Non-Small Cell Lung Cancer (NSCLCs), through non-canonical NF- $\kappa$ B activation<sup>13,14,26–28</sup>. However, many NSCLCs are resistant to death induced by BV6 and TNF, an observation that has limited the therapeutic efficacy of these compounds<sup>27,29,30</sup>. A potential mechanistic explanation for resistance of cancer cells to SMAC-mimetics emerged from our studies on *SIX*-proteins. Specifically, we identified three RAS and p53-driven NSCLC cell lines (H1155, H1792 and H2087) that were refractory to combined BV6/TNF induced cell death, and exhibited high levels of endogenous SIX1 and SIX2 protein (Fig. 4d, e). CRISPR-Cas9 knockout of *SIX1* and *SIX2* dramatically sensitized these NSCLCs to BV6/TNF (Fig. 4d, e). The anti-apoptotic function of *SIX*-proteins was also observed in SV40 immortalized fibroblasts and U-2 OS osteosarcoma cells (Extended Data Fig. 8, 9a–g). We confirmed that SIX1 and SIX2 suppressed Caspase-8 mediated cell death in these cell lines (Extended Data Fig. 9h–j).

To broadly investigate if the protective effects of *SIX*-proteins arise from regulation of gene expression programs, WT and *SIX1*<sup>-/-</sup> *SIX2*<sup>-/-</sup> H1792 NSCLCs were treated with BV6/TNF and processed for RNA-seq. Over 90% of the analyzed transcripts were unaltered by BV6/TNF treatment. However, of the 1024 genes induced greater than 2-fold (false discovery rate, FDR<0.05) by BV6/TNF treatment of WT cells, 120 were significantly upregulated in *SIX1*<sup>-/-</sup> *SIX2*<sup>-/-</sup> cells (cluster 1, Fig. 4f, Extended Data Fig. 10a and Table S4). Cluster 1 genes had a strong inflammatory response signature with enrichment of transcripts from cytokines and chemokines with experimentally verified  $\kappa$ B binding sites (Extended Data Fig. 10b). A large percentage of cluster 1 genes were also upregulated in unstimulated *SIX1*<sup>-/-</sup> *SIX2*<sup>-/-</sup> cells (Fig. 4f, Extended Data Fig. 10a, c), which is consistent with *SIX* promoter occupancy and inflammatory gene transcription profiles observed in non-cancer cells (Fig. 2f, 3a). In addition, *SIX*-proteins suppressed only a subset of  $\kappa$ B target genes as 78% of transcripts induced by BV6/TNF were unaltered between wild-type and *SIX1*<sup>-/-</sup> *SIX2*<sup>-/-</sup> (cluster 2, Fig. 4f and Table S5, 6). Together, these data provide an unbiased conformation that SIX1 and SIX2 regulate gene specific transcriptional responses induced by non-canonical NF- $\kappa$ B under both physiological and pathological conditions.

In summary, we have established that *SIX*-family transcription factors function as immunological gatekeepers, dampening the promoter activity of inflammatory genes in response to persistent non-canonical NF- $\kappa$ B pathway activation. In support of this mechanism, reactivation of SIX1 and SIX2 in immune cells is coupled to NIK protein accumulation caused by chronic cytokine stimulation or pathogen infection. In addition, expression of SIX1 and SIX2 directly inhibits the transactivation function of RelA and RelB in a negative feedback loop (Extended Data Fig. 6h). These findings not only connect the non-canonical NF- $\kappa$ B signaling pathway to a mechanism of transcriptional repression, but also indicate that disruption of this response circuit may have important consequences on the pathogenesis of human disease, including cancer<sup>1,4,5</sup>.

## METHODS

### Plasmids and reagents

Flag-tagged constructs were generated by cloning indicated genes into NotI and SalI sites of pCMV-6b-Flag backbone using Gibson Assembly Master Mix (E2611, NEB). RelA, and RelB were cloned into BamHI and NotI sites of pEBB-HA. GFP-tagged constructs were assembled by cloning indicated genes into EcoRI and BamHI sites of pEGFP-C2. NIK-stimulated genes and other indicated genes were cloned into TRIP.CMV.IVS $\beta$ .GENE.ires.TagRFP destination vector<sup>31</sup> using Gateway® LR Clonase™ II (11791, Invitrogen). The pRK5-HA-Ub plasmid was a gift from Ted Dawson (17608, Addgene). *GAL4-RelA* and *GAL4-LUC* plasmids<sup>23</sup> were kindly provided by Dr. Eric Olson (UT Southwestern Medical Center). *GAL4-RelB* was assembled by cloning full length RelB into EcoRI and XbaI using Gibson. NF- $\kappa$ B luciferase plasmid, containing 5 units of  $\kappa$ B enhancer elements, was obtained from Agilent technology (219077). NIK kinase dead (K429/430A)<sup>32</sup> and I $\kappa$ B<sup>SR</sup> (S32/36A)<sup>19</sup> mutants were generated by mutagenesis of indicated amino acids. All gene cloning was verified by sequencing.

Recombinant TNF (210-TA, R&D), LT $\alpha$ 1 $\beta$ 2 (L5162, Sigma) and TWEAK (SRP4360, Sigma) were reconstituted in sterilized PBS containing 0.1% BSA. LPS (L2880, Sigma) was reconstituted in sterilized double-distilled H<sub>2</sub>O. Doxycycline (D9891) was purchased from Sigma. BV6 (B4653, Apexbio), Z-VAD (FMK007, R&D), and Z-IETD (ALX-260-020-M001, Enzo) were dissolved in DMSO. X-tremeGENE9 transfection reagent was purchased from Roche. Following antibodies were used in this study: anti-Flag (A8592, Sigma), anti-Actin (A2066, Sigma), anti-HA (MMS-101P, Covance), anti-GFP (632592, Clontech), anti-pI $\kappa$ B $\alpha$  (2859, Cell Signaling), anti-I $\kappa$ B $\alpha$  (4814, Cell Signaling), anti-NIK (4994, Cell Signaling), anti-SIX1 (12891, Cell Signaling), anti-RelA (8242, Cell Signaling; sc-372x, Santa Cruz), anti-pRelA (3033, Cell Signaling), anti-RelB (sc-226x, Santa Cruz), anti-p100/52 (sc-7386, Santa Cruz), anti-H3 (ab1791, Abcam), anti-PARP (9542, Cell Signaling), anti-cleaved caspase-3 (9664, Cell Signaling), anti-TAK1 (MAB5307, R&D; #4505, Cell Signaling), anti-cIAP1 (AF8181, R&D) anti-SIX2 (11562-1-AP, Proteintech), anti-CD40 (ab13545, Abcam), anti-Pol II (39097, Active motif), and Rabbit normal IgG (12-370, Millipore).

### Mice, mice experiments, ELISA, peritoneal macrophages and BMDMs preparation

All mice in this study were bred and maintained under pathogen-free conditions in the animal care facility at UT Southwestern Medical Center. All experiments were performed according to experimental protocols approved by the Institutional Animal Care and Use Committee and complied with all relevant ethical regulations. *Nik*<sup>-/-</sup> mice were obtained from Jackson Laboratory (#025557)<sup>33</sup>. *Tet-O-HA-SIX1* embryos were kindly provided by Dr. Heide Ford (University of Colorado) and revived at UT Southwestern Medical Center transgenic core. Line #6239 was confirmed by PCR (primer sets are shown in Extended Data Fig. 7a)<sup>25</sup> and then intercrossed with *CAG-rtTA3* line (#016532, Jackson laboratory) to obtain the *rtTA3*<sup>+/-</sup> and *rtTA3*<sup>+/-</sup> *SIX1*<sup>+</sup> mice. Age- and gender-matched littermates were used for further experiments.

6–7 weeks old *rtTA3<sup>+/-</sup>* or *rtTA3<sup>+/-</sup> SIX1<sup>+</sup>* mice were given 2 mg/ml doxycycline water containing 10 g/L sucrose for 10 days (Dox water was refreshed 3–4 days). Mice were then injected with indicated dosage of LPS through intraperitoneal (I.P.) route. For survival and recovery assays, mice were monitored according to approved animal protocol and the survival rate was recorded at the indicated time post LPS injection. Mice were given a clinical score and then euthanized at the end point of experiment (96 hours post injection). Clinical score was given according to physical conditions induced by LPS including hunched posture, reduced mobility, ability to obtain food/water, and dehydration. The score range was from 0–9 (0: mouse was indistinguishable from untreated control, 9: mouse exhibited extreme sickness classified as moribund and was euthanized as the humane end point of the experiment). To measure Il-1 $\beta$  and Cxcl2 production, mice blood samples were collected and serum was isolated using 1.1ml Z-Gel microtube (41.1378.005, Sarstedt) at 4 hours post injection. Quantikine or DuoSet ELISA kit was used to measure the production of Il-1 $\beta$  (MLB00C, R&D) and Cxcl2 (DY452–005, R&D). Experiments were performed according to manufacturer's instructions. The absorbance units were measured by FLUOstar OPTIMA (BMG LABTECH).

Peritoneal macrophages were isolated from *rtTA3<sup>+/-</sup>* and *rtTA3<sup>+/-</sup> SIX1<sup>+</sup>* mice as described previously<sup>34</sup>. Briefly, mice were euthanized by CO<sub>2</sub>. 7–8 ml sterilized cold PBS was injected into cavity through peritoneal wall. Cell suspension fluid was aspirated from peritoneum and pelleted using 1000 $\times$ g for 3 minutes. Cells were then seeded in poly-lysine pretreated 12-well-plate and cultured in DMEM media in the presence or absence of 2  $\mu$ g/ml doxycycline. After 24 hours, adherent cells were used for LPS administration.

To obtain primary bone marrow derived macrophages (BMDMs), bone marrow cells were collected from 6-week-old wild type C57BL/6NJ, *Nik<sup>-/-</sup>*, *rtTA3<sup>+/-</sup>* or *rtTA3<sup>+/-</sup> SIX1<sup>+</sup>* mice' femurs and tibiae. Red cells were eliminated by applying 1 $\times$ RBC buffer (TNB-4300-L100, TONBO biosciences). Cells were then cultured and differentiated in DMEM supplemented with 10% FBS and 10% conditional media of L929 cell culture for 6–7 days. 2 $\times$ 10<sup>5</sup> differentiated primary BMDM cells were seeded in 12-well-plate for *Lm* infection, cytokines treatment, or LPS administration. All cells were grown at 37 $^{\circ}$ C in a 5% CO<sub>2</sub> incubator.

## Cell lines

SV40-immortalized *STAT1<sup>-/-</sup>* fibroblasts were kindly provided by Dr. Jean-Laurent Casanova, Rockefeller University and were cultured in RPMI (Gibco) supplemented with 10% FBS and 1 $\times$ NEAA. HCT116 (ATCC), U-2 OS (ATCC), HEK293A (Jack Dixon, University of California, San Diego) and HEK293T (Paul Bieniasz, Aaron Diamond AIDS Research Center) cells were cultured in DMEM (Gibco) supplemented with 10% FBS (Gibco or Sigma) and 1 $\times$ NEAA (Gibco). NSCLC cell lines H1155 (KRAS<sup>A183T(Q61H)</sup>), TP53<sup>G818A(R273H)</sup>, PIK3CA<sup>C2529G(D843E)</sup>, DDR2<sup>C187T(L63L, splice site)</sup> and PTEN<sup>C697T(R233\*)</sup>, H2087 (NRAS<sup>C181A(Q61K)</sup>), TP53<sup>G469T(V157F)</sup>, ALK<sup>T1657G(S553A)</sup>, and BRAF<sup>C1789G(L597V)</sup>, and H1792 (KRAS<sup>G34T(G12C)</sup> and TP53<sup>splice site</sup>) were kindly provided by Dr. John Minna (UT Southwestern Medical Center) and were cultured in RPMI

supplemented with 10% FBS and 1×NEAA. Indicated knock out or stable cell lines were generated as described below. All cells were grown at 37°C in a 5% CO<sub>2</sub> incubator.

### Lentivirus production and transduction

For lentivirus production, 4×10<sup>5</sup> HEK293T cells were seeded in each well of poly-lysine coated 6-well-plate. 1 µg of indicated lentiviral expressing genes, 0.8 µg HIV gag-pol, and 0.2 µg vesicular stomatitis virus glycoprotein (VSV-G) were transfected into HEK293T cells by X-tremeGENE 9. The transfection media was replaced with fresh DMEM/3% FBS/1×NEAA after 6 hours. Lentiviral particles were collected at 48 hours and 72 hours. Pooled supernatants were cleared by centrifugation at 1500 rpm for 5 minutes. Supernatants, supplied with 20mM HEPES and 4 µg/ml polybrene, were stored in -80°C.

For lentivirus transduction, 7×10<sup>4</sup> fibroblasts, HEK293A or U-2 OS cells were seeded in each well of 24-well-plate. Cells were transduced with indicated lentivirus in transduction media (RPMI or DMEM supplemented with 3% FBS, 20 mM HEPES and 4 µg/ml polybrene) by spinning 1000×g for 45 minutes at 37°C. The transduction media was replaced with culture media after 6 hours. Transduced cells were split into duplicate after 48 hours transduction, followed by bacteria and virus infection assay.

### Bacteria and virus infection

To generate GFP expressing *Shigella*, *Shigella flexneri* M90T was transformed with pBBRMCS1-GFP plasmid. GFP expressing *Listeria monocytogenes* 10403s strain was a gift from Dan Portnoy (University of California, Berkeley). For *Shigella* infection, bacteria were grown in BHI broth media (237500, BD science) supplemented with 5 µg/ml chloramphenicol (CAM) at 30°C with 200 rpm shaking for overnight. Bacteria were then diluted 1:25 into BHI/5 µg/ml CAM and incubated at 37°C for about 2 hours (OD<sub>600</sub>~0.5). Bacteria were washed with PBS and then suspended in PBS/0.03% Congo red (C6277, Sigma) and incubated at 37°C for 15 minutes. Bacteria (MOI of 10:1) suspensions were inoculated to each well of 24-well-plate, followed by centrifugation at 1000×g for 10 minutes. Infected cells were then incubated at 37°C in a 5% CO<sub>2</sub> incubator for 1.5 hours. Extracellular bacteria were killed by replacing the media supplemented with 50 µg/ml gentamicin. After 8 hours incubation, cells were collected for flow cytometry analysis. For *Listeria* infection, bacteria were cultured overnight in BHI at 30°C without shaking and (MOI of 10:1) suspensions were inoculated to each well of 24-well-plate (for U-2 OS cells, centrifugation at 1000×g for 7 minutes was performed to help *Listeria* adhesion) and incubated for 1.5 hours. Cells were then incubated for 4.5 hours after replacing with gentamicin-contained media.

Viral infection was performed as previous described<sup>9</sup>. Briefly, all viruses were suspended in RPMI media supplemented with 1% FBS/1×NEAA. Cells were infected by adding 200 µl virus suspensions to each well of 24-well-plate (MOI of 0.5:1) and then incubated after adding 800 µl RPMI media supplemented with 10% FBS/1×NEAA for the indicated time periods: EAV (19 hours, 1 hour infection+18 hours incubation), WINV (25 hours, 1+24), PIV3 (16 hours, 3+13), and SINV (10 hours, 1+9).

## Flow Cytometry and data analysis

To quantify bacterial and viral infection efficiency, infected cells were detached by 37°C warmed Accumax (Sigma), followed by centrifugation at 800×*g* for 2 minutes. Cells were then fixed by suspending in PBS/1% PFA at 4°C for at least 30 minutes. Cells were then stored in PBS/3% FBS. The Stratadigm S1000 flow cytometry was used to distinguish the RFP-, BFP-, or GFP-expressed cells. All flow cytometry generated raw data was analyzed by FlowJo 10.0.6. For most part of analysis, we gated live cells, single cell population from live cells, and then RFP positive cells from single cell population. Finally, we gated the GFP positive units from RFP positive population. For RFP-, BFP-, or GFP-expressed experiments, we gated cells that expressed both RFP and BFP to analyze GFP expressed population.

## CRISPR-Cas9 gene editing cell lines

The *RelA*, *RelB*, *NIK*, *TAK1*, or *SIX1/SIX2* guide RNA (the guide targets both *SIX1* and *SIX2* genes) was cloned into lenti-CRISPR v2 vector<sup>35</sup> (Dr. Feng Zhang, Addgene 52961) according to the protocol. Lentivirus was produced as described above. 7×10<sup>4</sup> fibroblasts, U-2 OS, H1155, H1792, or H2087 cells were transduced with indicated lentivirus and incubated for 48 hours. Transduced cells were then selected with 2 µg/ml (fibroblasts and U-2 OS) or 5 µg/ml (H1155, H1792, and H2087) puromycin for 7 days. Single colony cells were sorted by flow cytometry. Homozygote knockout cells were then determined by genotyping and western blot. Knock out of *SIX1* and *SIX2* in H1155, H1792, and H2087 resulted from a single T insertion to both alleles as shown in Extended Data Fig. 4c.

## *Lm* infection-, cytokines and LPS stimulation- and drug treatment-induced *SIX*-proteins accumulation

For *Lm*-, cytokines-, LPS or drug-induced endogenous *SIX1* and *SIX2* protein accumulation, 1×10<sup>5</sup> WT, *NIK*<sup>-/-</sup>, *TAK1*<sup>-/-</sup> fibroblasts or 2×10<sup>5</sup> primary BMDM cells (WT and *Nik*<sup>-/-</sup>) were seeded in 12-well-plate. Cells were then infected with *Lm* (MOI=0.1 [BMDMs]), or treated with 25 ng/ml TNF, 50 ng/ml LTα1β2, 100 ng/ml LPS, 50 ng/ml TWEAK, 30 µM MG132 or 5 µM BV6 for 24 hours or the indicated time. The whole cells were then lysed in lysis buffer (50 mM Tris-HCl pH7.6, 150 mM NaCl, 1% Triton X-100, and 1×protease inhibitor, cocktail) along with 1×laemmli sample buffer (161–0737, Biorad). Whole cell lysates were then separated by 8% SDS-PAGE and probed with indicated antibodies by western blot. The same method was applied to the entire study unless otherwise stated in the figure legend (e.g. Fig. 2d and Extended Data Fig. 3m, 6a). For MG132 treatment, indicated cells were challenged with 30 µM MG132 for 12 hours or the indicated time. To analyze RelA and RelB translocation, the cell plasma membrane was disrupted by incubation in lysis buffer (50 mM Tris-HCl pH7.6, 150 mM NaCl, 1% NP-40, and 1×protease inhibitor, cocktail). Nuclei were pelleted by centrifugation and cytosolic extracts were collected for analysis. Nuclei were then washed 2–3 times with lysis buffer and were boiled in lysis buffer to obtain nuclear extracts. 12% SDS-PAGE was used to separate H3.

For BV6-, or MG132-induced CMV-Flag-*SIX2* protein accumulation, indicated plasmids were transfected into 5×10<sup>4</sup> HEK293T cells. After 24 hours transfection, cells were treated

with 5  $\mu\text{M}$  BV6 or 30  $\mu\text{M}$  MG132 for 24 or 12 hours. For NIK expression induced SIX1 and SIX2 accumulation, GFP-SIX1/SIX2 were co-transfected with Flag-NIK into HEK293T cells. SIX1 and SIX2 expression was quantified by fluorescence microscopy and western blot after 48 hours transfection. To test BV6/TNF-induced apoptosis pathway activation,  $1 \times 10^5$  fibroblasts were seeded in 12-well-plate. Cells were then treated with 25 ng/ml TNF plus 2.5  $\mu\text{M}$  BV6 along with or without 30  $\mu\text{M}$  z-VAD or 40  $\mu\text{M}$  z-IETD for 6 hours. 12% SDS-PAGE was used to separate cleaved caspase-3.

### Immunoprecipitation assay

To test the interaction between SIX2 and RelA/RelB,  $8 \times 10^5$  HEK293T cells were transfected with the indicated plasmids (6 $\mu\text{g}$  total). After 48 hours, cells were lysed in 1 ml lysis buffer, followed by 30s on and 30s off sonication for 7–10 cycles to break the nuclei. Anti-Flag immunoprecipitation was carried out using anti-Flag M2 affinity gel (A2220, Sigma) for 4 hours. Beads were then washed 4 times with lysis buffer. Co-immunoprecipitated proteins were separated by SDS-PAGE and the present proteins were detected by anti-HA or Flag western blot.

For ubiquitination of SIX2, Flag-*SIX2* and HA-Ub were co-transfected with EV or GFP-*NIK* into HEK293T cells. After 48 hours, equal amount of Flag-SIX2 proteins were loaded for anti-Flag immunoprecipitation. Ubiquitinated SIX2 were detected by anti-HA western blot.

### Yeast two hybrid

To test the interaction between SIX2 and RelA *trans*-activation domain, full-length SIX2 was cloned into the pACT2-AD vector. Amino acid 473–522 of RelA, which does not have ability of self-activation<sup>36</sup>, was cloned into pLexNA-BD vector. Yeast transformation was performed using standard LiAc based method. Equal amount of indicated yeast cells were placed on either SD/UWL<sup>-</sup> or SD/WHULK<sup>-</sup> (Clontech) with 10  $\mu\text{M}$  3-Amino Triazole (3-AT) and grown for 2–3 days.

### RNA sequencing and data analysis

RNA sequencing (RNA-seq) was performed at UTSW McDermott Center Next Generation Sequencing Core and analyzed at the McDermott Center Bioinformatics Lab as described previously<sup>37</sup>. Briefly, *Fluc* or *NIK* lentivirus was transduced into WT fibroblasts. After 72 hours, total RNA was purified according to RNAeasy mini kit instruction (QIAGEN, 74104) and prepared according to the TruSeq® stranded mRNA sample preparation guide (Illumina). Sequencing data was then generated by Illumina HiSeq 2500 by reading paired-end 100 bp (base pair). To consider the NIK-stimulated genes, each read was mapped to human genome based on Human-hg19 by Tophat (v2.0.10) based on igenome annotations (<https://ccb.jhu.edu/software/tophat/igenomes.shtml>). Cufflinks/Cuffdiff (v2.1.1) was then used to calculate the expression value of each sample and identify differentially expressed genes in *Fluc* or *NIK* sample using a regularized t-test<sup>38</sup>. Only genes with  $\log_2(\text{fold change; FC}) \geq 1$  or  $\leq -1$  and false discovery rate (FDR) < 0.05 were considered as NIK up- or down-regulated genes compare to *Fluc* control.

To analyze the SIX2-downregulated NIK-stimulated genes, *Fluc<sup>RFP</sup>/Fluc<sup>BFP</sup>*, *NIK<sup>RFP</sup>/Fluc<sup>BFP</sup>*, *NIK<sup>RFP</sup>/SIX2<sup>BFP</sup>*, or *Fluc<sup>RFP</sup>/SIX2<sup>BFP</sup>* lentivirus was transduced into WT fibroblasts. RNA purification and RNA sequencing were performed as described above. Comparison of *NIK/SIX2* vs *NIK/Fluc* (comp I) or *NIK* vs *Fluc* (comp II) was carried out by considering  $\log_2(\text{FC}) \geq 1$  or  $\leq -1$  and  $\text{FDR} < 0.01$ . The SIX2 downregulated NIK-stimulated genes were then adjusted by comparing comp I with comp II.

For BV6/TNF-induced gene transcription profiles in H1792 NSCLCs,  $3 \times 10^5$  WT and *SIX1<sup>-/-</sup> SIX2<sup>-/-</sup>* cells were treated with mock or 5  $\mu\text{M}$  BV6 along with 25 ng/ml TNF for 24 hours. The total RNA was extracted from the adherent cells. RNA sequencing was performed as described above. The read length for this experiment is 75 bp single-end. To analyze the differential expression profiles, fastq files were checked for quality using fastqc (v0.11.2; <http://www.bioinformatics.babraham.ac.uk/projects/fastqc>) and fastq\_screen (v0.4.4; [http://www.bioinformatics.babraham.ac.uk/projects/fastq\\_screen](http://www.bioinformatics.babraham.ac.uk/projects/fastq_screen)) and were then quality trimmed using fastq-mcf (ea-utils/1.1.2-806)<sup>39</sup>. Trimmed fastq files were mapped to hg19 (UCSC version from igenomes) using TopHat<sup>40</sup>, duplicates were marked using picard-tools (v1.127 <https://broadinstitute.github.io/picard/>), read counts were generated using featureCounts<sup>41</sup> and differential expression analysis was performed using the generalized linear model likelihood ratio test implemented in edgeR<sup>42</sup>. For comparison of BV6/TNF-induced genes in WT cells, only gene that exhibits  $\log_2(\text{counts per million}) \geq 1$ ,  $\log_2(\text{FC}) \geq 1$ , and  $\text{FDR} < 0.05$  was considered as up-regulated genes. The differential genes between BV6/TNF-treated WT and *SIX1<sup>-/-</sup> SIX2<sup>-/-</sup>* cells were considered by  $\log_2\text{FC} \geq 1$  (up) or  $\leq -1$  (down) and  $\text{FDR} < 0.05$ . The remaining genes were considered as no change. The expression levels of each of the 1,024 differentially expressed genes were normalized across conditions to generate z-scores and presented in Fig. 4f. Final gene lists were then used for pathway analysis with QIAGEN's Ingenuity Pathway Analysis tool (QIAGEN Redwood City, <http://www.qiagen.com/ingenuity>). Trends in these gene lists were also plotted using various R packages (<https://www.R-project.org/>). The significance values for the canonical pathways are calculated by one-sided Fisher's exact test.

### RNA-seq data validation and qRT-PCR

To validate RNA-seq data, experiments were performed as described above. Briefly, total RNA was isolated for synthesizing cDNA using SuperScriptIII First-Strand Kit (18080051, Invitrogen). The gene expression level was quantified by real-time PCR through detecting the SYBR green (4309155, ABI) by ABI 7500 fast real-time PCR system. To test if SIX1 and SIX2 suppressed NIK-stimulated genes and if these NIK-stimulated genes were dependent on RelA or RelB, WT, *RelA<sup>-/-</sup>*, *RelB<sup>-/-</sup>*, or *SIX1<sup>-/-</sup> SIX2<sup>-/-</sup>* fibroblasts were transduced with *Fluc* or *NIK* lentivirus. Total RNA was isolated after 72 hours transduction. Gene expression level was quantified by qRT-PCR.

For *Lm*- and TNF-stimulated *Six1* and *Six2* gene expression,  $2 \times 10^5$  WT and *Nik<sup>-/-</sup>* primary BMDM cells were seeded in 12-well-plate and then infected with *Lm* (MOI $\approx$ 0.1) or treated with 25 ng/ml TNF for 24 hours. For TWEAK-induced *IL-1 $\beta$* , *IL-8*, and *CCL3* gene transcription in fibroblasts, WT and *SIX1<sup>-/-</sup> SIX2<sup>-/-</sup>* fibroblasts were treated with 50 ng/ml TWEAK for 24 hours. For LPS-induced inflammatory mediators' gene expression in

peritoneal macrophages, cells were treated with 100 ng/ml LPS for 4 hours. Relative gene expression was adjusted to housekeeping gene  $\beta$ -*Actin* (murine or human) and then normalized to experimental control.

### NIK-stimulated genes library

Based on the RNA-seq data, 273 genes were identified as NIK-stimulated genes. 237 out of 273 genes were cloned into the TRIP.CMV.IVS $\beta$ .GENE.ires.TagRFP destination vector. 141 genes were obtained from hORF Collection (Invitrogen), 35 were from DNASU<sup>43</sup> and 61 were from the type I interferon library<sup>31</sup>. Lentiviruses were produced as described above.

### Luciferase reporter assay

$1 \times 10^4$  HEK293T cells or  $2 \times 10^4$  WT, *RelA*<sup>-/-</sup>, or *RelB*<sup>-/-</sup> fibroblasts were seeded in each well of 48-well-plate. Indicated plasmids were transfected into cells along with *LacZ* (as transfection control) and  $5 \times \kappa B$ -*LUC*, *pIL-8-LUC*, or  $5 \times GAL4$ -*LUC* and incubated for 48 hours. For cytokines treatment, after 24 hours transfection, cells were treated with 25 ng/ml TNF or 50 ng/ml LT $\alpha$ .1 $\beta$ 2 for 24 hours. Activity of luciferase was measured according to manufacturer's protocol (E1500, Promega). ONPG buffer (2-Nitrophenyl  $\beta$ -D-galactopyranoside dissolving in 200 mM NaH<sub>2</sub>PO<sub>4</sub>, 2 mM MgCl<sub>2</sub>, and 100 mM  $\beta$ -mercaptoethanol) was used to measure activity of *LacZ*. The luminescence and absorbance units were measured by FLUOstar OPTIMA (BMG LABTECH). Relative luciferase activity was quantified by adjusting to *LacZ* control and normalizing to experimental control.

### Fluorescence microscopy

To analyze localization of truncated SIX2 fragments,  $2 \times 10^4$  U-2 OS cells were seeded on coverslips in 24-well-plate. Indicated Flag-tagged *SIX2* fragments were transfected into cells. After 48 hours, cells were washed 2–3 times with PBS and were fixed by incubating in 500  $\mu$ l PBS/3.7% formaldehyde for 10 minutes at 37°C, followed by washing 3 times with PBS and incubation in 500  $\mu$ l PBS/50 mM NH<sub>4</sub>Cl for 10 minutes. Cells were permeabilized in PBS/10% horse serum/0.5% Triton X-100 for 45 minutes. Cells were then incubated with primary antibody (1:500 anti-Flag in PBS/10% horse serum/0.5% Triton X-100) for 45 minutes. After washing 3 times with PBS, secondary antibody (1:500 fluorescein conjugated goat anti-mouse from Pierce and 1:1000 DAPI in PBS/10% horse serum/0.5% Triton X-100) was added and incubated for 45 minutes. After washing 3 times with PBS and 1 time with H<sub>2</sub>O, the samples were mounted on slides and images were processed by Zeiss Observer Z1 fluorescent microscope.

### Chromatin-immunoprecipitation

GFP-SIX1 stable cell line was generated by cloning *GFP-SIX1* into pSCRPSY-blasticidin backbone. Lentiviruses were produced as described above. Fibroblasts and HCT116 cells were transduced and selected by using 10  $\mu$ g/ml blasticidin. Positive cells were used for following experiments. Chromatin-immunoprecipitation (Ch-IP) assay was performed according to manufacturer's instructions (Millipore, 12–495). Briefly,  $1.0 \times 10^7$  cells were cross-linked by 1% PFA for 10 minutes at 37°C and 125 mM glycine was used to quench crosslinking. Cells were then washed with chilled PBS twice, and lysed in lysis buffer (5mM

PIPES pH8.0, 85mM KCl, 0.5% NP-40, 1mM PMSF, 1×protease inhibitor). The nuclei were then pelleted down by spinning at 3,000 rpm for 5 minutes and were resuspended in RIPA buffer (50 mM Tris-HCl pH8.0, 1% NP-40, 150 mM NaCl, 0.5% Sodium Deoxycholate, 0.1% SDS, 2.5 mM EDTA, 1 mM PMSF, 1×protease inhibitor). Nuclei lysates were sonicated 40 cycles (HCT116 cells, 70 cycles for fibroblasts) with 30s on and 30s off to yield fragments of 200–1000 bps using Bioruptor (Diagenode). 6 µg of IgG, SIX1, RelA or Pol II antibodies were conjugated with the protein G beads (10004D, Invitrogen) for 1 hour and blocked using 5% BSA for 1 hour. After spinning down sonicated nuclei lysates at 13,000 rpm for 10 minutes, equal supernatant of sonication products was incubated with the pre-conjugated protein G beads at 4°C overnight. The bound beads were washed with RIPA buffer, low salt buffer, high salt buffer, and LiCl buffer once, finally with TE buffer twice. The bound protein-DNA complex was eluted by 500 µl elution buffer (100 mM NaHCO<sub>3</sub>, 1% SDS). 20 µl 5 M NaCl was added to reverse crosslinks of protein and DNA by heating at 65°C for over 4 hours or overnight. DNA was recovered by PCA and precipitated by ethanol in the presence of glycogen (AM9515, Invitrogen). The enrichment of *IL-1β*, *IL-8*, and *CCL3* promoter was measured by quantitative PCR (qPCR). Fold enrichment was normalized to experimental control. For RelA and Pol II ChIP experiments, fold enrichment was adjusted to “input DNA” that was saved prior to immunoprecipitation and then normalized to experimental control.

### Cell viability assay

$5 \times 10^3$  (for 48 hours treatment) or  $1 \times 10^4$  (for 24 hours treatment) indicated cells were seeded in the 96 well plates (Costar, black with clear flat bottom, 3603). After 19 hours, the media was removed and fresh media supplemented with the indicated compounds were added and incubated at 37°C with 5% CO<sub>2</sub> for 24 or 48 hours. Whole cell ATP levels were measured using CellTiter Glo following manufacturer’s instructions (G7572, Promega). The luminescence units were measured by FLUOstar OPTIMA (BMG LABTECH). For SIX2 complementation assays,  $7 \times 10^4$  parental, *NIK*<sup>-/-</sup> or *SIX1*<sup>-/-</sup> *SIX2*<sup>-/-</sup> fibroblasts were seeded in the 24-well-plate. Then cells were transduced with *Fluc*, *SIX2* or *SIX2<sup>R</sup>* lentivirus. After 50 hours, transduced cells were seeded in 96 well plates and the experiments were performed as described above.

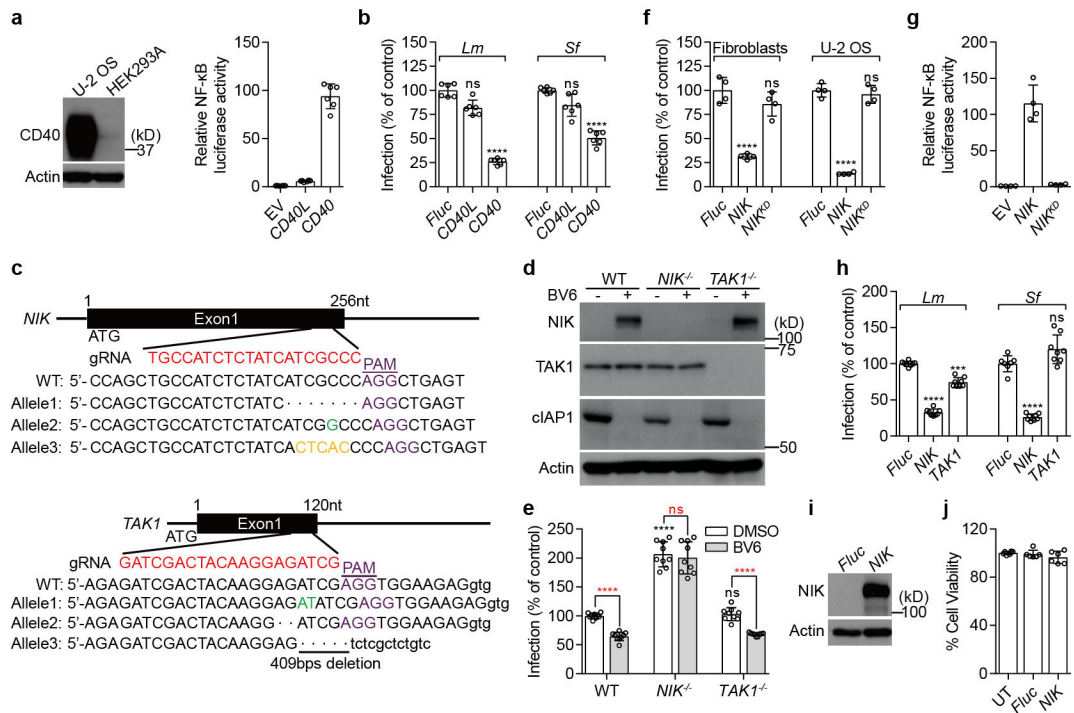
### DATA AVAILABILITY

All data generated during this study that supporting the findings are included in the manuscript or in its source data and supplementary information. All materials are available from authors upon reasonable request. The RNA-seq data associated with Fig. 4f, Extended Data Fig. 2b, and Extended Data Fig. 4g have been deposited in NCBI (insert accession code when it is available).

### Supplementary Material

Refer to Web version on PubMed Central for supplementary material.

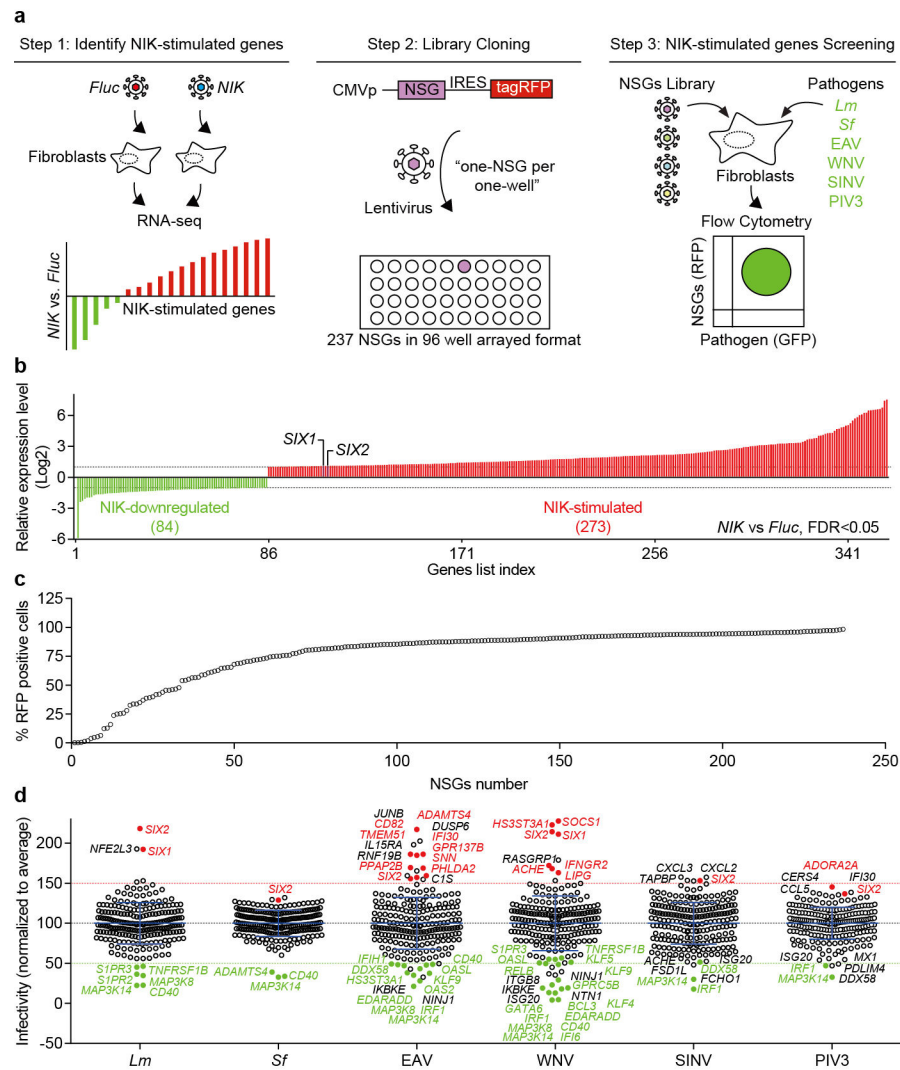
### Extended Data



### Extended Data Fig. 1. CD40-NIK signaling axis mediates anti-bacterial function.

**a, b**, Experiments were performed to exclude the possibility that the observed CD40L induced anti-bacterial function was specific to a particular cell type or protocol of cytokine induction. We reconstituted the CD40L signaling pathway in HEK293 cells. These cells do not express CD40, the endogenous receptor for CD40L (**a**, western blot). HEK293 cells are also unable to be stimulated by CD40L (**a**, graph). However, we found that overexpression of CD40 strongly induced NF-κB pathway activation (**a**, graph). Expression of CD40 restricted both *Lm* and *Sf* infection (**b**) to levels similar to those observed in CD40L treated U-2 OS cells (compare data to Fig. 1b). The NF-κB reporter activity assay in panel **a** was performed by co-transfecting empty vector (EV), *CD40L* or *CD40* with 5×κB-*LUC* reporter gene into HEK293T cells. Luciferase activity was measured after 48 hours and normalized to EV (right). Data are mean±s.d. from 6 independent experiments. Experiment and quantification of panel **b** is presented as in Fig. 1b. Data are mean±s.d. from 6 independent experiments. **c, d**, Conformation of genetic knockout of the *MAPK3K14* (here forward referred to as *NIK*) and *MAPK3K7* (here forward referred to as *TAK1*) genes in *STAT1*<sup>-/-</sup> human fibroblasts. **c**, Schematic representation of In/Del base pairing and the sgRNA targets locus of Exon 1 in the *NIK* and *TAK1* gene. *NIK*<sup>-/-</sup> contains -7bps, +G, and +CTCAC alleles (top). *TAK1*<sup>-/-</sup> contains +AT alleles, -2bps, and -409bps (bottom). (- means deletion, + means insertion). **d**, Western blot shows endogenous NIK and TAK1 expression in parental, *NIK*<sup>-/-</sup> and *TAK1*<sup>-/-</sup> cells. It is important to point out that NIK is constitutively degraded by cIAPs-TRAF2/3 E3-ligase complex in quiescent cells<sup>2</sup>. To detect NIK expression, WT, *NIK*<sup>-/-</sup>, and *TAK1*<sup>-/-</sup> fibroblasts were treated with 2.5 μM BV6 (a SMAC-mimetics compound that antagonizes cIAPs and leads to NIK accumulation<sup>13,14</sup>) for 14 hours and then the endogenous proteins were probed with indicated antibodies by western blot. **e**, NIK is necessary for restricting *Lm* infection. Fibroblasts with the indicated genetic

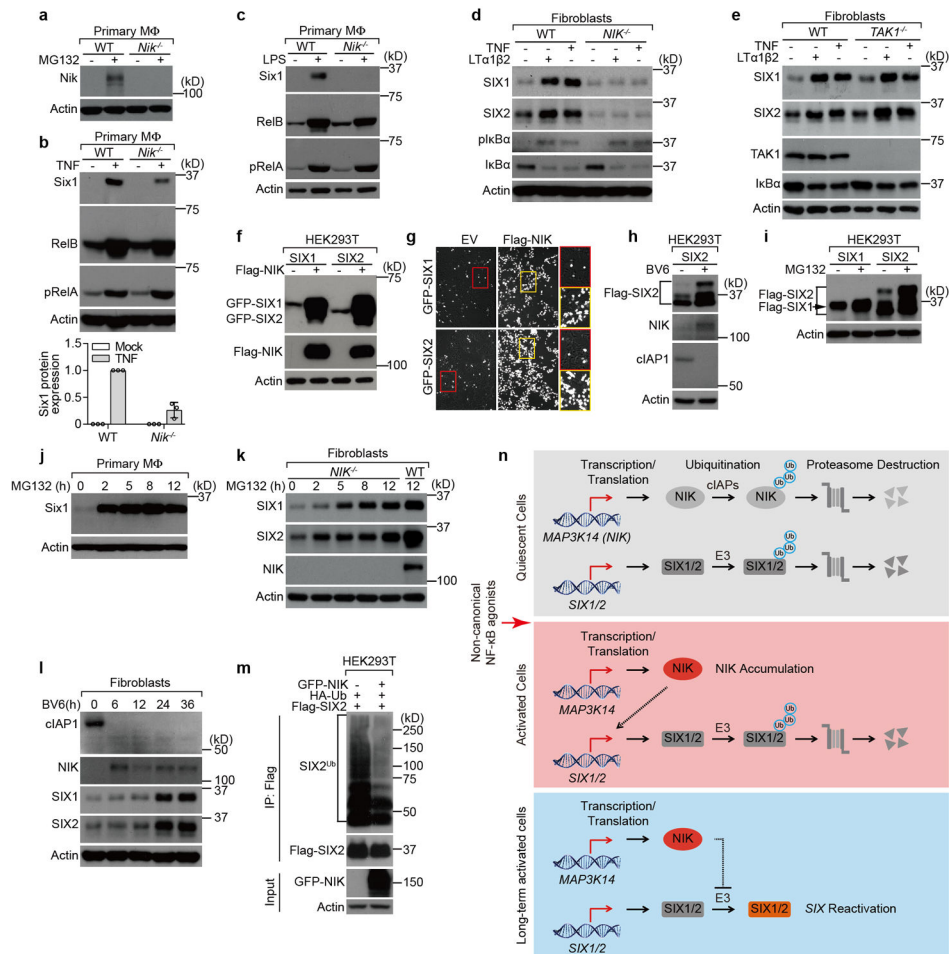
background were treated with vehicle control (DMSO) or 2.5  $\mu$ M BV6 for 14 hours and then infected with *Lm*<sup>GFP</sup>. The percent of bacterial infection was normalized to WT uninfected control. Black statistic markers denote the difference between WT and indicated cell lines and red markers denote the difference between DMSO and BV6 treatment. We noted that *NIK*<sup>-/-</sup> cells exhibited much greater levels of *Lm* infection than either WT or *TAK*<sup>-/-</sup> cells consistent with its role in preventing infection after cellular stimulation. However, BV6 treatment of cells, which suppressed *Lm* infection of WT cells, had no effect on *NIK*<sup>-/-</sup> cells further indicating that NIK activation is necessary for the anti-bacterial response. Data are mean $\pm$ s.d. from 9 independent experiments. **f**, The kinase activity of NIK is required for its anti-bacterial function. *Fluc*, WT *NIK* or NIK-kinase dead mutant (*NIK*<sup>K429/430A</sup> referred to as *NIK*<sup>KD</sup>) lentivirus was transduced into fibroblasts or U-2 OS cell as indicated. Cells were then challenged with *Sf*<sup>GFP</sup>. Quantification of bacterial infection is presented as described in Fig. 1b. Data are mean $\pm$ s.d. from 4 independent experiments. **g**, NF- $\kappa$ B gene expression induced by NIK is kinase dependent. Empty vector (EV), *NIK* or *NIK*<sup>KD</sup> was co-transfected with 5 $\times$  $\kappa$ B-*LUC* into HEK293T cells. NF- $\kappa$ B activity was measured after 48 hours and normalized to EV (right). Data are mean $\pm$ s.d. from 4 independent experiments. **h**, Expression of NIK, but not TAK1, potentially inhibits *Lm* and *Sf* infection. WT U-2 OS cells were transduced with combinational *Fluc*<sup>RFP</sup>/*Fluc*<sup>BFP</sup>, *NIK*<sup>RFP</sup>/*Fluc*<sup>BFP</sup>, or *TAK1*<sup>RFP</sup>/*TABI*<sup>BFP</sup> lentivirus. Cells were then challenged with *Lm*<sup>GFP</sup> or *Sf*<sup>GFP</sup>. Infection efficiency was quantified by flow cytometry. The infection efficiency was determined by gating GFP positive cells in both RFP and BFP positive cell populations. The relative percentage of pathogen infection was normalized to *Fluc* control. Data are mean $\pm$ s.d. from 8 independent experiments. **i**, Control experiment showing NIK protein expression levels that correspond to experiments presented in Fig. 1c. *Fluc* and *NIK* transduced cells were lysed and probed with anti-NIK antibody. **j**, Overexpression of NIK does not cause cytotoxicity in fibroblasts. Previous studies suggest that ectopic expression of NIK causes cytotoxicity in A549 cells<sup>44</sup>. To test if ectopic expression of NIK causes cytotoxicity in fibroblasts, we transduced WT fibroblasts with indicated lentivirus and measured the cell viability after 72 hours by measuring ATP. Data are mean $\pm$ s.d. from 6 independent experiments. *P* values were measured using one-way ANOVA (GraphPad), \*\*\**P*<0.001, \*\*\*\**P*<0.0001, ns: no significant difference. The same statistics were used in the later figures unless otherwise stated. Western blot data are representative of 3 independent experiments. For gel source data, see Supplementary Figure 1.



### Extended Data Fig. 2. NIK-stimulated genes library screen.

**a**, Schematic of NIK-stimulated gene library design, cloning, and the multidimensional flow cytometry based high throughput screen. NIK-stimulated genes were determined by RNA-seq. The cDNAs of 237 NIK-stimulated genes were individually cloned into the lentiviral vector pTRIP upstream of the IRES-tagRFP (see methods). Fibroblasts were transduced with lentivirus in a one-gene to one-well format and were then infected with GFP expressing *Lm*, *Sf*, EAV, WNV, SINV, and PIV3 in independent experiments. The effect of a single gene expression on infection was quantified by flow cytometry. **b**, The relative expression levels of NIK-stimulated genes identified by RNA-seq. *Fluc* or *NIK* lentivirus was transduced into fibroblasts. Total RNA was isolated after 72 hours and gene expression level was determined by RNA sequencing. Graph shows gene expression levels that are significantly stimulated (red, 237 genes) or downregulated (green, 84 genes) by *NIK* expression compared to *Fluc* control. Fold change over 2 ( $\text{Log}_2 = 1$ ) or less 0.5 ( $\text{Log}_2 = -1$ ) and  $\text{FDR} < 0.05$  (statistics test is presented in methods section). Bars were ranked numerically from low to high (see Table S1 for details). The expression levels of *SIX1* and *SIX2* are indicated. Data are representative of 2 independent experiments. **c**, Graph showing

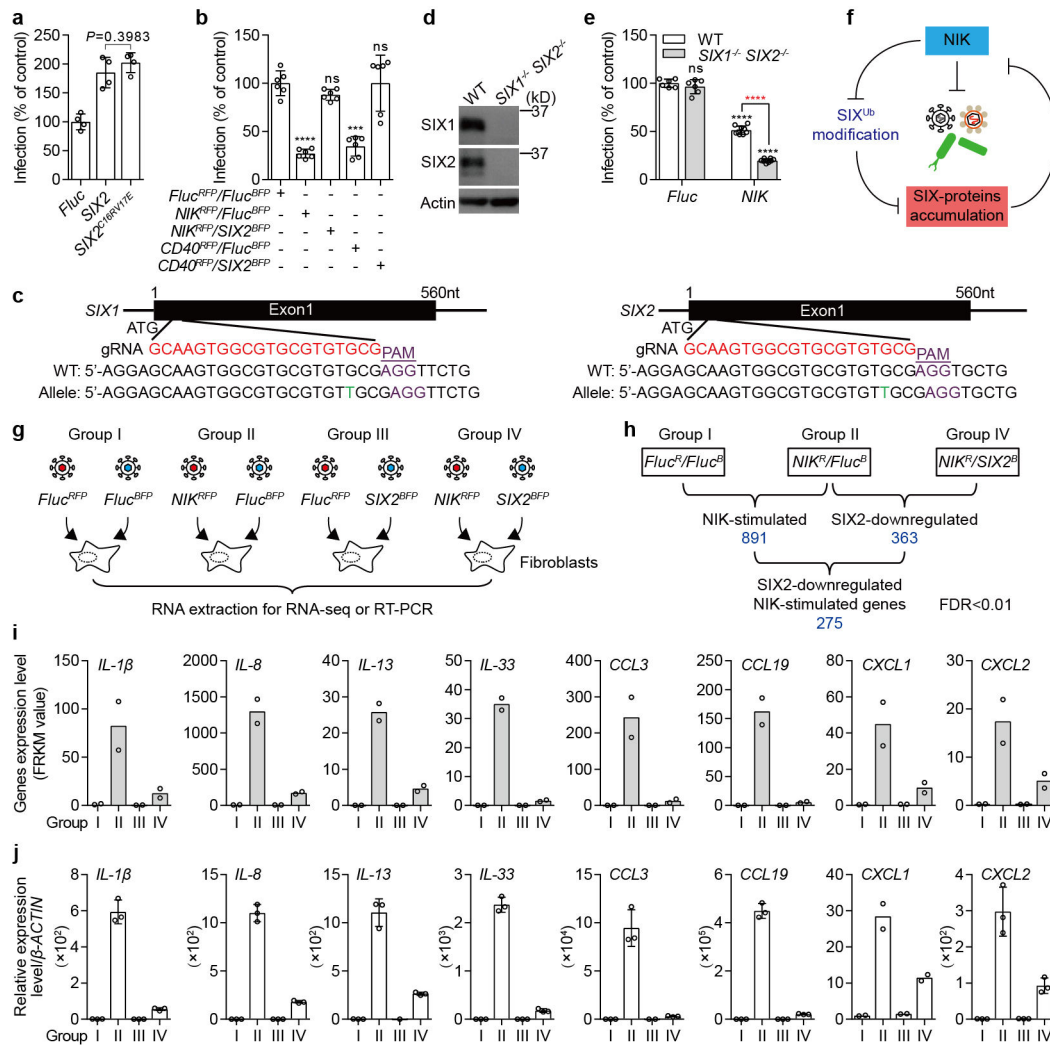
the efficiency of lentiviral expression of NIK-stimulated genes used in the high throughput bacterial and viral screen. NIK-stimulated genes were transduced into WT fibroblasts in a “one-gene per one-well” format. Transduction efficiency as measured % RFP positive cells was determined by flow cytometry and was ranked numerically from low to high (see source data for details, values are from the average of 2 technical replicates). 12 out of 237 genes were poorly transduced (less than 20% RFP+) and were excluded from subsequent analyses. **d**, Dot plots of *Sf*, *Lm*, EAV, WNV, SINV, and PIV3 infectivity in the presence of expressed NIK-stimulated genes (in c). Data were normalized to the average of each screen, indicating as the black dotted line. We chose to confirm hits in Fig. 1d based on two criteria: (1) the gene expression effect on inhibiting or enhancing pathogen infection by less than or greater than 50%, and (2) an adjusted Z-score less than -2 or greater than 2 (see Table S2 for details). NIK-stimulated genes that reproducibly and significantly inhibited (green) or enhanced infection (red) by these criteria are indicated. The genes shown in black font are hits that were not reproduced in the confirmatory experiments (Fig. 1d). Data are mean±s.d. from 2 (*Sf* and *Lm*) or 1 (EAV, WNV, SINV, and PIV3) independent experiments.



### Extended Data Fig. 3. NIK mediates reactivation of SIX-proteins by inhibiting the ubiquitin/proteasome pathway.

**a**, Control experiment for Fig. 2a, c showing that Nik is expressed in WT BMDMs but not in BMDMs isolated from *Map3k14*<sup>-/-</sup> (here forward *Nik*<sup>-/-</sup>) mice. As mentioned in Extended Data Fig. 1d, Nik protein is constitutively degraded under quiescent condition. Thus, we employed MG132 proteasome inhibitor to stabilize endogenous Nik protein expression. To validate Nik protein expression, WT and *Nik*<sup>-/-</sup> primary BMDM cells were treated with mock or 30 μM MG132 for 12 hours and Nik protein was detected by western blot. **b**, **c**, Long term treatment of cells with TNF (**b**) or LPS<sup>45</sup> (**c**) stabilized Six1 expression through activation of Nik in murine primary BMDM cells. WT and *Nik*<sup>-/-</sup> primary BMDMs were treated with 25 ng/ml TNF (**b**, graph showing quantification of Six1 protein expression in TNF treated cells mean±s.d. from 3 independent experiments as described in Fig. 2c) or 100 ng/ml LPS (**c**) for 24 hours. **d**, **e**, Human SIX1 and SIX2 protein reactivation by long term treatment of cells with both canonical (TNF) and non-canonical (LTα1β2) NF-κB agonists requires NIK, but not TAK1. WT, *NIK*<sup>-/-</sup> or *TAK1*<sup>-/-</sup> fibroblasts were treated with mock, 25 ng/ml TNF or 50 ng/ml LTα1β2 for 24 hours. LTα1β2 was employed as positive control of a non-canonical NF-κB agonist. *TAK1*<sup>-/-</sup> cells were included as control to show TNF and LTα1β2 could induce SIX1 and SIX2 accumulation in a TAK1 independent manner (**e**). **f**, **g**, Ectopic expression of NIK induces expression of recombinant SIX1 and SIX2 driven by the

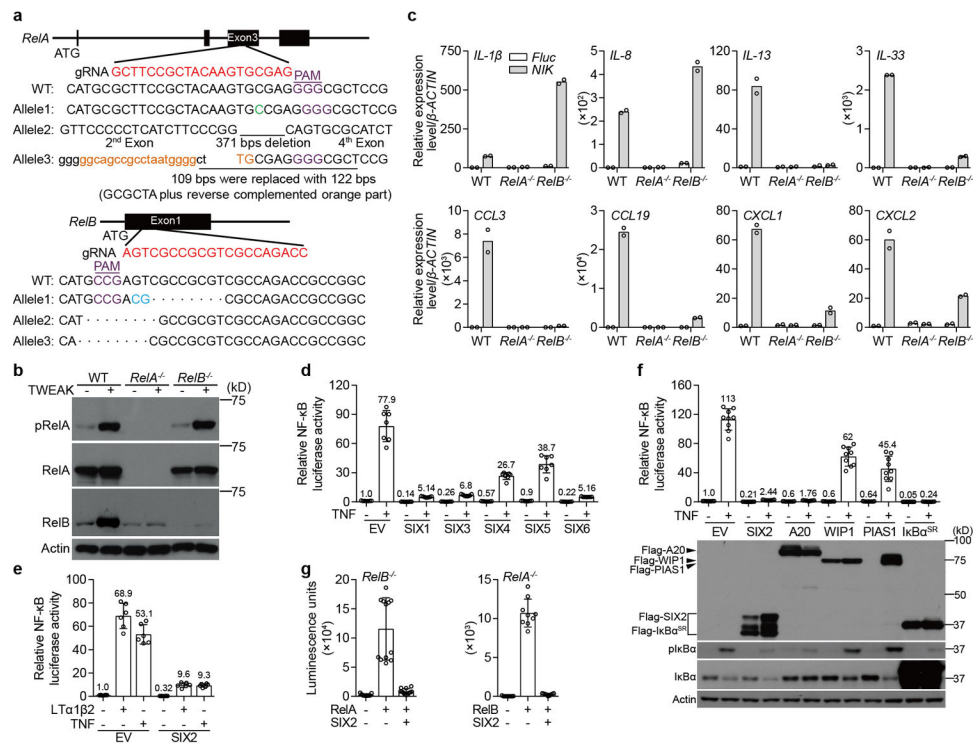
strong CMV promoter in HEK293 cells. Plasmids encoding CMV-driven GFP-SIX1 or GFP-SIX2 were co-transfected into HEK293T cells with empty vector (EV) or Flag-NIK. Western blot (f) and fluorescence microscopy (g) assays were performed to detect expression of GFP-SIX1 and GFP-SIX2 post 48 hours transfection. We estimate that SIX1 and SIX2 protein are expressed in 5–10% of untreated cells, whereas they are expressed in 60–70% of cells when co-transfected with NIK. Microscopy images were taken using a 10× objective (g). **h, i**, Experiments showing that activation of NIK by BV6 (h) or by inhibition of the proteasome with MG132 (i) stabilizes CMV-Flag-SIX2 expression in HEK293T cells. Flag-*SIX2* was transfected into HEK293T cells for 24 hours, cells were then treated with mock or 5 μM BV6 for 24 hours or 30 μM MG132 for 12 hours. **j**, Inhibition of the 26S proteasome with MG132 induces endogenous Six1 protein expression in primary BMDMs. Cells were treated with 30 μM MG132 for the indicated time. **k**, Inhibition of the 26S proteasome promotes SIX1 and SIX2 expression in human fibroblasts and this expression occurs in *NIK*<sup>-/-</sup> fibroblasts. Experiments were performed as in j. **l**, Kinetics of cIAP1 degradation and NIK, SIX1 and SIX2 accumulation in human fibroblasts treated with BV6. WT fibroblasts were treated with 5 μM for indicated time. **m**, NIK potently suppresses SIX2 ubiquitination. HEK293T cells were co-transfected with HA-ubiquitin and Flag-*SIX2* along with GFP-*NIK* as indicated and cells were incubated for 48 hours. SIX2 was immunoprecipitated with anti-Flag antibody. The ubiquitination status of the protein was determined by anti-HA western blot. **n**, Diagram showing the reactivation mechanism of *SIX*-proteins in response to non-canonical NF-κB activation. Details are explained in the main text. All data are representative of 3 independent experiments. For gel source data, see Supplementary Figure 1.



#### Extended Data Fig. 4. SIX-proteins oppose NIK-mediated anti-bacterial function through inhibiting NIK-stimulated genes expression.

**a**, SIX2 enhances bacterial infection independent of interaction with Eya family transcriptional co-activators. Previous studies have shown that SIX-family transcription factors assemble gene co-activator complexes through interaction with Eyes Absent (Eya) family members<sup>17</sup>. Structural studies indicate that SIX1 residues C16 and V17 are required for the interaction with EYA2<sup>18</sup>. These residues are conserved in SIX2. Thus, using mutant  $SIX2^{C16RV17E}$  protein, we found that SIX2 enhances *Lm* infection independent of EYA interactions. *Fluc*, WT *SIX2*, or  $SIX2^{C16RV17E}$  lentivirus was transduced into WT fibroblast cells. Cells were then challenged with *Lm*<sup>GFP</sup>. The percent of *Lm* infection was normalized to *Fluc* control. Data are mean $\pm$ s.d. from 4 independent experiments. *P* is shown in the figure. **b**, Expression of SIX2 suppresses the anti-microbial function of NIK and CD40. WT fibroblasts were lentiviral transduced with a combination of cDNAs (*Fluc*<sup>RFP</sup>/*Fluc*<sup>BFP</sup>, *NIK*<sup>RFP</sup>/*Fluc*<sup>BFP</sup>, *NIK*<sup>RFP</sup>/*SIX2*<sup>BFP</sup>, *CD40*<sup>RFP</sup>/*Fluc*<sup>BFP</sup>, or *CD40*<sup>RFP</sup>/*SIX2*<sup>BFP</sup>). After 72 hours, cells were infected with *Lm*<sup>GFP</sup>. The RFP-, BFP- and GFP-expressed cells were gated by flow cytometry. Quantification of infection was performed as described in Extended Data Fig. 1h. Data are mean $\pm$ s.d. from 6 independent experiments. \*\*\**P*<0.001, \*\*\*\**P*<0.0001,

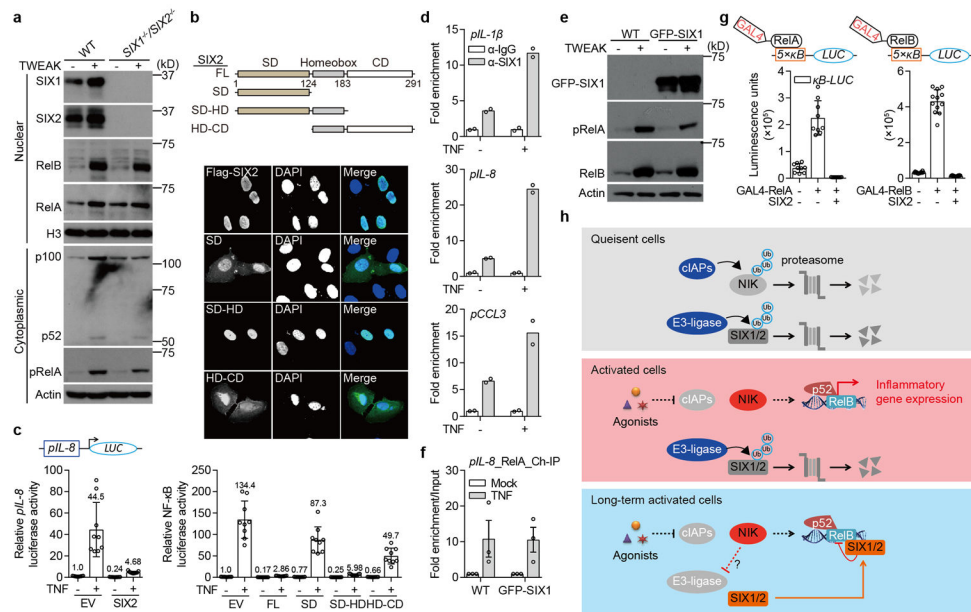
ns: no significant difference. **c, d**, Characterization of *SIX1*<sup>-/-</sup> *SIX2*<sup>-/-</sup> fibroblasts generated by CRISPR-Cas9. Schematic representation of In/Del base pairing and the sgRNA targets locus of Exon 1 in the *SIX1* and *SIX2* gene in fibroblasts (c). *SIX1*<sup>-/-</sup> *SIX2*<sup>-/-</sup> contains a single T insertion in both alleles of the *SIX1* and *SIX2* genes. Western blot shows endogenous *SIX1* and *SIX2* expression in parental and *SIX1*<sup>-/-</sup> *SIX2*<sup>-/-</sup> fibroblasts (d). Data are representative of 3 independent experiments. **e**, The anti-bacterial activity of *NIK* is enhanced in *SIX1*<sup>-/-</sup> *SIX2*<sup>-/-</sup> fibroblasts. WT and *SIX1*<sup>-/-</sup> *SIX2*<sup>-/-</sup> fibroblasts were transduced with *Fluc* or *NIK* lentivirus. After 72 hours, cells were then challenged with *Lm*<sup>GFP</sup>. Black statistic markers denote the difference between WT (*Fluc*) and WT (*NIK*) or *SIX1*<sup>-/-</sup> *SIX2*<sup>-/-</sup> (*Fluc* or *NIK*). Red marker denotes the difference between WT (*NIK*) and *SIX1*<sup>-/-</sup> *SIX2*<sup>-/-</sup> (*NIK*). Relative infectivity was normalized to WT (*Fluc*) control. These data indicate that *SIX*-proteins oppose the function of *NIK*, potentially through suppression of non-canonical NF- $\kappa$ B gene expression (see f, below). Data are presented as mean $\pm$ s.d. from 6 independent experiments. \*\*\*\**P*<0.0001, ns: no significant difference. **f**, Model illustrating the relationship between *NIK* expression, *SIX*-proteins accumulation, and their roles in regulating anti-microbial immunity. **g**, Diagram describing RNA-seq experiments used to identify *NIK*-stimulated genes that are suppressed by *SIX2*. To identify the *NIK*-stimulated genes that are regulated by *SIX2*, the indicated lentiviruses (group I-IV) were transduced into WT fibroblasts. Total RNA was extracted for deep sequencing post 72 hours transduction (see Table S3). **h**, Diagram showing the group comparisons from data generated in g. Briefly, the *NIK*-stimulated genes that suppressed by *SIX2* were determined from Group IV vs Group II comparison (Log<sub>2</sub> -1) and then adjusted to *NIK*-stimulated genes that are from Group II vs Group I comparison (we chose fold change greater than 4), FDR<0.01 (statistics test is presented in methods section). **i**, Representative raw data from RNA-seq experiments performed in g, h. RNA-seq data are presented as FPKM value (bars show mean from 2 independent experiments indicated as circle). **j**, Validation of RNA-seq data. Experiments were performed as described as in g. Gene transcription level was determined by qRT-PCR and relative gene expression was normalized to *Fluc* control. Data are mean $\pm$ s.d. of 3 or 2 technical replicates and representative of 3 independent experiments. For gel source data, see Supplementary Figure 1.



### Extended Data Fig. 5. *SIX*-family proteins inhibit RelA and RelB mediated NF-κB activation.

**a, b**, Characterization of *RelA*<sup>-/-</sup> and *RelB*<sup>-/-</sup> in human fibroblasts. Schematic representation of In/Del base pairing and the sgRNA targeting locus of Exon 3 in *RelA* and Exon 1 in *RelB* gene. *RelA*<sup>-/-</sup> cells contain +C, -371 bps, and a 109 bps fragment that was replaced with 122 bps containing the GCGCTA with reverse complementary (orange fragment) (a up). *RelB*<sup>-/-</sup> cells contain the indicated deletions (a bottom). Western blot shows endogenous RelA and RelB expression in parental and *RelA*<sup>-/-</sup> or *RelB*<sup>-/-</sup> fibroblasts and response to stimulation by 24-hour application of TWEAK (b). **c**, Experiments evaluating the contributions of the canonical and non-canonical NF-κB subunits RelA and RelB, respectively, on expression of the indicated genes. *Fluc* or *NIK* was transduced into WT, *RelA*<sup>-/-</sup>, and *RelB*<sup>-/-</sup> fibroblasts to stimulate the non-canonical NF-κB signaling pathway and mRNA expression of the indicated genes were evaluated by qRT-PCR. We concluded that the *IL-1β* gene is specifically stimulated by RelA since we did not detect its expression in *RelA*<sup>-/-</sup> cells but did so in *RelB*<sup>-/-</sup> cells (which expression RelA). Similar logic was used to evaluate the 7 additional genes shown. Experiments were performed as described in Fig. 2g. Bars are mean of 2 technical replicates (shown as circle) and representative of 2 independent experiments. **d**, The human *SIX*-family consists of 6 unique isoforms. To determine which of these genes suppress NF-κB mediated gene expression, empty vector (EV), *SIX1*, *SIX3*, *SIX4*, *SIX5*, or *SIX6* cDNAs were co-transfected with 5×κB-*LUC* into HEK293T cells. After 24 hours, cells were treated with mock or 25 ng/ml TNF for 24 hours. The luciferase activity was measured and normalized to EV untreated control. *SIX1*, *SIX3*, and *SIX6* (*SIX2* was not evaluated in this experiment) potently inhibited both basal and inducible activity of NF-κB. Data are mean±s.d. from 7 independent experiments. **e**, *SIX2* inhibits LTα1β2- and TNF-induced NF-κB activation. EV

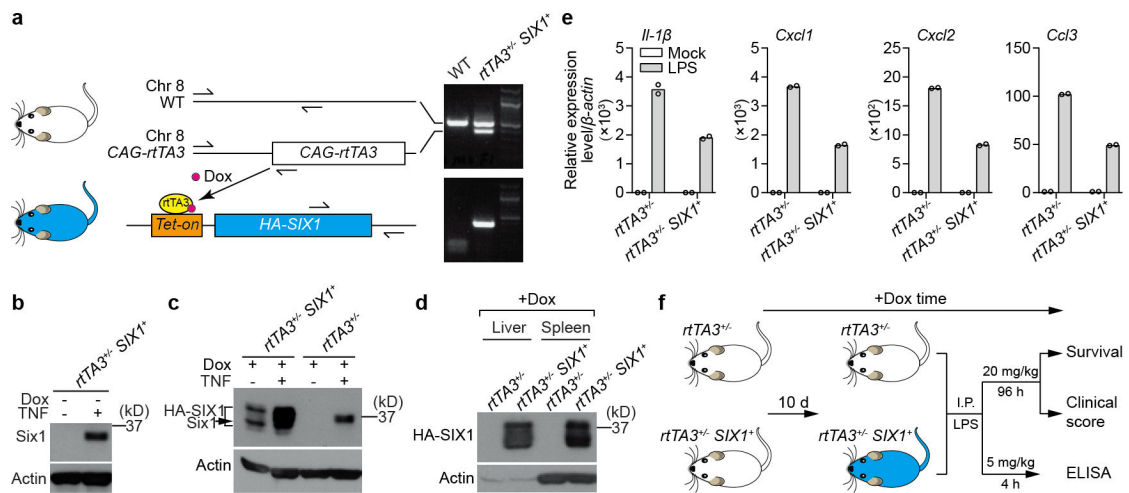
or Flag-*SIX2* was co-transfected with  $5\times\kappa B$ -*LUC* into WT fibroblasts. After 24 hours, cells were treated with mock, 25 ng/ml TNF or 50 ng/ml  $LT\alpha.1\beta 2$  for 24 hours. Data were analyzed as described in d. Data are mean $\pm$ s.d. from 6 independent experiments. **f**, The inhibitory potency of *SIX2* is equivalent to A20 and  $I\kappa B\alpha^{SR}$ . The Flag-tagged genes indicated were co-transfected with  $5\times\kappa B$ -*LUC* into HEK293T cells. After 24 hours, cells were treated with mock or 25 ng/ml TNF for 24 hours. Data were analyzed as in d. Data are mean $\pm$ s.d. from 9 independent experiments. Anti-Flag western blot was performed to determine expression levels,  $I\kappa B\alpha$  regulation was included as pathway activation control upon cellular stimulation with TNF. **g**, Experiments showing that *SIX2* specifically inhibits the activity of both canonical and non-canonical NF- $\kappa B$  isoforms RelA and RelB, respectively. To evaluate the transcriptional activity of each NF- $\kappa B$  isoform independently, we transfected *RelA* cDNA into *RelB*<sup>-/-</sup> cells and *RelB* cDNA into *RelA*<sup>-/-</sup> cells along with *SIX2*,  $5\times\kappa B$ -*LUC*. Transfection of both *RelA* and *RelB* potently induced NF- $\kappa B$  transcription of the indicated cells, and this transcription was suppressed by *SIX2*. Luminescence units were measured post 48 hours transfection. Data are mean $\pm$ s.d. from 12 (left) and 9 (right) independent experiments. All western blot data are representative of 3 independent experiments. For gel source data, see Supplementary Figure 1.



**Extended Data Fig. 6. *SIX*-family proteins inhibit NF- $\kappa$ B activation through occupying the target gene promoters.**

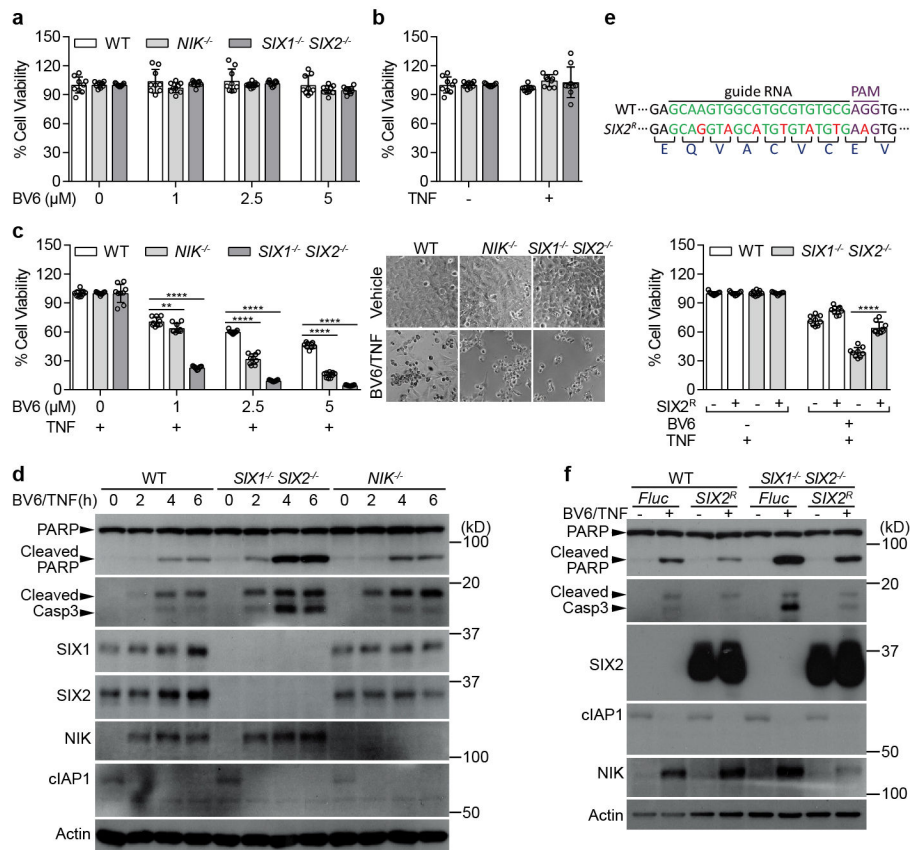
**a**, In order to narrow down the possible mechanisms for *SIX*-proteins inhibition of inflammatory gene expression, we monitored the activation, processing and nuclear translocation of RelA and RelB upon cellular stimulation with TWEAK. WT and *SIX1<sup>-/-</sup>SIX2<sup>-/-</sup>* H1792 cells were treated with mock or 50 ng/ml TWEAK for 24 hours. Cells lysates from cytoplasmic or nuclear fractions were analyzed by western blot. Neither SIX1 nor SIX2 blocked RelA phosphorylation, p100/52 processing, or restricted NF- $\kappa$ B translocation to the nucleus. **b**, Domain analysis of *SIX*-family protein function. *SIX*-proteins are composed of a Six Domain (SD), Homeobox domain (HD), and Coiled Coil (CD) region (diagram). Full-length SIX1 and SIX2 have 80% identical amino acids over the entirety of the protein coding sequence. The SD and HD domains (residues 1–183, highlighted) are 96% identical<sup>46</sup>. The indicated FLAG-tagged *SIX2* fragments were transfected alone into U-2 OS cells and processed for microscopy (middle) or transfected with 5 $\times$   $\kappa$ B-*LUC* into HEK293T cells and processed for  $\kappa$ B reporter activity (bottom). The highly conserved SD-HD domain was the minimal fragment that inhibited  $\kappa$ B reporter activity. This fragment strictly localized to the nucleus, together indicating that *SIX*-proteins inhibit nuclear activity of NF- $\kappa$ B. Graph data were analyzed as described in Extended Data Fig. 5d. Data are mean  $\pm$  s.d. from 9 independent experiments. **c**, *SIX2* inhibits gene activation from the *IL8*-promoter. *pIL8-LUC* plasmid composed of the 1.5 kilobase (kb) promoter region of *IL-8* cloned upstream of luciferase gene, was co-transfected with indicated plasmids into HEK293T cells. After 24 hours, cells were treated with mock or 25 ng/ml TNF for 24 hours. The luciferase activity was then measured and analyzed as described in Extended Data Fig. 5d. Data are mean  $\pm$  s.d. from 9 independent experiments. Together, these data suggested that *SIX*-proteins inhibit NF- $\kappa$ B activation at gene promoters. **d**, Chromatin immunoprecipitation (ChIP) experiment providing additional evidence that *SIX*-proteins bind to inflammatory gene promoters as shown in Fig. 3a. Chromatin was prepared from GFP-SIX1 stable cell lines (HCT116 cells) treated with mock or 25 ng/ml

TNF for 2 hours. Anti-SIX1 antibodies (or anti-IgG control) were used to immunoprecipitate SIX1 from nuclear extracts. Co-eluted DNA was amplified by primer sets as shown in Fig. 3a. Relative promoter occupancy was normalized to each experimental IgG control. Bars are mean of 2 technical replicates (shown as circles) and data are representative of 3 independent experiments. **e**, Control experiments corresponding to Fig. 3a and Extended Data Fig. 6f showing GFP-SIX1 expression levels. WT and GFP-SIX1 stable fibroblasts were stimulated with 50 ng/ml TWEAK for 24 hours. GFP-SIX1 expression was measured by western blot. **f**, SIX1 expression does not affect recruitment of RelA to the *IL-8* promoter. Chromatin was prepared from WT or GFP-SIX1 stable fibroblasts and then immunoprecipitated with anti-RelA. Bound DNA was amplified and quantified by qPCR. Results were adjusted to “input DNA” that was saved prior to immunoprecipitation. Relative enrichment was then normalized to each group’s untreated control. Data are presented as mean±s.d. from 3 independent experiments. **g**, Control experiments corresponding to Fig. 3c showing that SIX2 inhibits GAL4-RelA and GAL4-RelB induced  $5\times\kappa B$ -*LUC* activity. To validate if GAL4-RelA and GAL4-RelB constructs were functional, GAL4 DNA-binding domain fused RelA or RelB construct was co-transfected with indicated plasmids into HEK293T cells. 48 hours post transfection, the luminescence units were measured. Data are mean±s.d. from 9 (left) and 12 (right) independent experiments. **h**, Model showing NIK-mediated reactivation of *SIX*-proteins function in a negative feedback loop to control inflammatory gene expression by targeting gene promoter and inhibiting NF- $\kappa$ B *trans*-activation function. In quiescent cells (top panel), NIK and *SIX*-proteins are constitutively ubiquitinated and degraded by the proteasome. Non-canonical NF- $\kappa$ B agonists (e.g. TWEAK, LT $\alpha$ 1 $\beta$ 2, or BV6) promote degradation of cIAPs, loss of NIK ubiquitination and subsequent NIK protein accumulation (middle panel). Stabilized NIK protein activates non-canonical NF- $\kappa$ B mediated inflammatory gene expression (middle panel). Under conditions of long-term cytokine exposure, NIK-mediated suppression of a currently unknown E3-ubiquitin ligase results in *SIX*-protein accumulation (bottom panel). Consequently, *SIX*-proteins suppress inflammatory gene expression by targeting gene promoters and directly inhibiting NF- $\kappa$ B *trans*-activation function in a negative feedback loop (bottom panel). All western blot and microscopy data are representative of 3 independent experiments. For gel source data, see Supplementary Figure 1.



### Extended Data Fig. 7. Doxycycline-induced *HA-SIX1* expression in mice.

**a**, Schematic representation of the doxycycline-induced *HA-SIX1* bitransgenic mouse model system. *CAG-rtTA3* mice were intercrossed with Tet-on driven *HA-SIX1* mice to obtain *rtTA3<sup>+/-</sup>-SIX1<sup>+</sup>* mice. In principle, doxycycline bound *rtTA3* targets the Tet-on operator and drives broad *HA-SIX1* expression across multiple tissues. Primer sets used to genotype *CAG-rtTA3* on chromosome 8 and Tet-on *HA-SIX1* are shown. Electrophoresis gels shows genotyping of a representative *rtTA3<sup>+/-</sup>-SIX1<sup>+</sup>* bitransgenic mouse. **b**, Anti-SIX1 western blot of whole cell lysates from BMDMs isolated from *rtTA3<sup>+/-</sup>-SIX1<sup>+</sup>* mice. *HA-SIX1* is not expressed in the absence of doxycycline under quiescent condition (left lane). *TNF* was administered to these cells as a control showing that endogenous murine *Six1* is stimulated in these cells (right lane). **c**, Whole cell lysates from doxycycline treated BMDMs isolated from *rtTA3<sup>+/-</sup>* or *rtTA3<sup>+/-</sup>-SIX1<sup>+</sup>* mice. BMDMs were stimulated with *TNF*, as indicated, and probed with anti-SIX1 antibody by western blot. Dox induced *HA-SIX1* expression (lane 1), and this induction is potentiated by *TNF* (lane 2). We noted that *HA-SIX1* ran as a doublet, which potentially represents unmodified and a mono-ubiquitinated form of the *SIX1* protein. Neither endogenous *Six1* nor *HA-SIX1* was detected in BMDMs isolated from Dox treated *rtTA3<sup>+/-</sup>* mice (lane 3). In control experiments, *TNF* induced endogenous murine *Six1* in BMDMs isolated from Dox treated *rtTA3<sup>+/-</sup>* mice (lane 4). **d**, *HA-SIX1* is expressed in liver and spleen. *rtTA3<sup>+/-</sup>-SIX1<sup>+</sup>* and *rtTA3<sup>+/-</sup>* mice were given 2 mg/ml doxycycline through drinking water for 10 days. Cell lysates from liver and spleen were used to probe *HA-SIX1* expression by anti-SIX1 western blot. All western blot data are representative of 3 independent experiments. **e**, Peritoneal macrophages were isolated from *rtTA3<sup>+/-</sup>-SIX1<sup>+</sup>* and *rtTA3<sup>+/-</sup>* littermate control mice. The adherent macrophages were incubated with 2  $\mu$ g/ml doxycycline for 24 hours and then treated with mock or 100 ng/ml LPS for 4 hours. Total RNA was isolated for RT-qPCR. Relative gene expression was normalized to *rtTA3<sup>+/-</sup>* untreated control. Bars show mean from 2 technical replicates (shown as circles). Data are representative of 3 independent experiments. **f**, Diagram showing the experimental procedures corresponding to Fig. 4a–c. Further experimental details are provided in the methods section. For gel source data, see Supplementary Figure 1.



**Extended Data Fig. 8. *NIK*<sup>-/-</sup> and *SIX1*<sup>-/-</sup> *SIX2*<sup>-/-</sup> sensitized fibroblasts to BV6/TNF induced cell death.**

To further validate the observation that *SIX1*<sup>-/-</sup> *SIX2*<sup>-/-</sup> sensitized NSCLCs cell lines to combined BV6 and TNF induced cell death, we chose SV40 immortalized *STAT1*<sup>-/-</sup> fibroblasts for additional studies. **a, b**, Fibroblasts of the indicated genotype were treated with either BV6 (a) or TNF (b) alone. Cell viability was determined by measuring ATP after 24 hours. Cell survival rate was normalized to each genotype untreated control. Neither BV6 nor TNF (10ng/ml) alone induced fibroblast cell death. **c**, Knockout of *NIK* or *SIX1/SIX2* sensitized fibroblasts to combined BV6/TNF induced cell death. Experiments were performed and data were analyzed as in (a) (graph). Representative images showing that the cell death phenotype induced by BV6/TNF in fibroblasts of the indicated genotype (right panels). **d**, Time course of combined BV6 (2.5 μM) and TNF (25 ng/ml) treatment of the indicated fibroblast genotypes. *NIK*<sup>-/-</sup> and *SIX1*<sup>-/-</sup> *SIX2*<sup>-/-</sup> cells exhibited increased cleavage of poly ADP-ribose polymerase (PARP) and the executioner Caspase-3 in BV6/TNF treated fibroblasts. We also noted that BV6/TNF induced *NIK*-dependent expression of both *SIX1* and *SIX2* proteins suggesting this cascade may be responsible for resistance to this treatment. **e, f**, We introduced a silent mutations in gRNA recognition sequence of the *SIX2* cDNA that cannot be targeted by CRISPR-Cas9 (*SIX2*<sup>R</sup>, e, diagram). Expression of *SIX2*<sup>R</sup> in *SIX1*<sup>-/-</sup> *SIX2*<sup>-/-</sup> fibroblasts rescued the cell death phenotype (e) and suppressed both PARP and Caspase-3 cleavage (f) induced by BV6/TNF. WT and *SIX1*<sup>-/-</sup> *SIX2*<sup>-/-</sup> fibroblasts were transduced with *Fluc* or *SIX2*<sup>R</sup> lentivirus. After 72 hours, cells were treated with mock or 0.2 μM BV6 plus 10 ng/ml TNF for 24 hours and cell

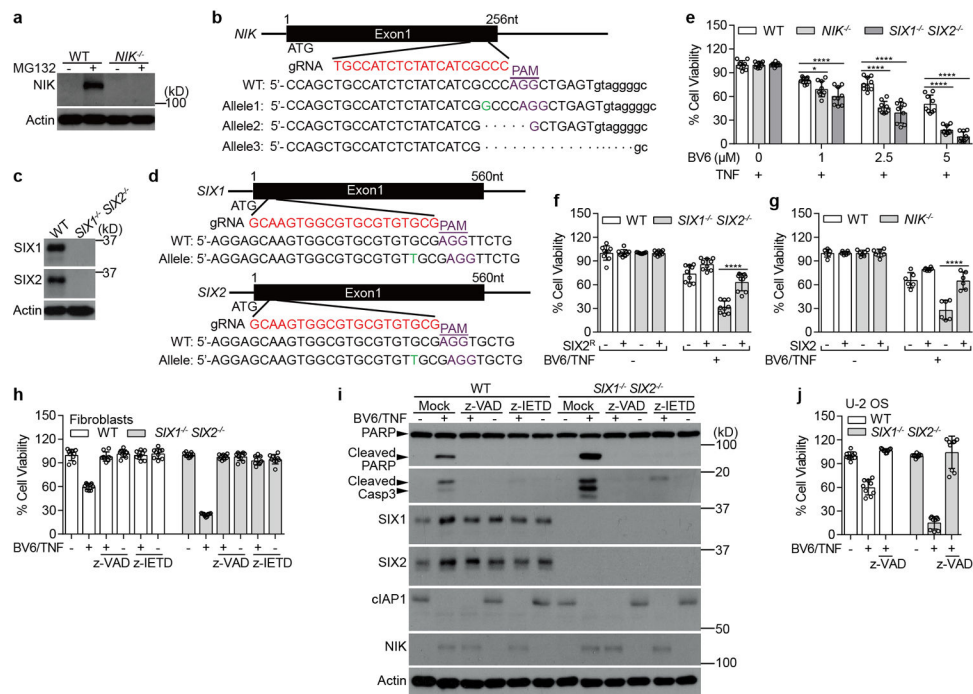
viability was determined by measuring ATP. Cell survival rate was normalized to each untreated control (e, bottom). For western blot, cells were treated with 2.5  $\mu$ M BV6 plus 25 ng/ml TNF for 6 hours (f). All quantified data are mean $\pm$ s.d. from 9 independent experiments. \*\* $P$ <0.01, \*\*\*\* $P$ <0.0001. Western blot data are representative of 3 independent experiments. For gel source data, see Supplementary Figure 1.

Author Manuscript

Author Manuscript

Author Manuscript

Author Manuscript



**Extended Data Fig. 9. *NIK*<sup>-/-</sup> and *SIX1*<sup>-/-</sup>*SIX2*<sup>-/-</sup> sensitized U-2 OS cells to BV6/TNF induced caspase-8-dependent cell death.**

**a-d**, Knock out *NIK* or *SIX1*/*SIX2* in U-2 OS cells using the CRISPR-Cas9 system. Western blot shows endogenous *NIK*, *SIX1*, or *SIX2* expression in parental, *NIK*<sup>-/-</sup> and *SIX1*<sup>-/-</sup>*SIX2*<sup>-/-</sup> U-2 OS cells (a, c). We employed MG132 to stabilize endogenous *NIK* protein in WT and *NIK*<sup>-/-</sup> U-2 OS cells. Schematic representation of In/Del base pairing and the sgRNA targets locus of Exon 1 in the *NIK* in U-2 OS cells (b). *NIK*<sup>-/-</sup> contains +G, -5bps, and -18 bps (disrupted the alternative splicing site) alleles. Schematic representation of In/Del base pairing and the sgRNA targets locus of Exon 1 in the *SIX1* and *SIX2* gene in U-2 OS cells (d). *SIX1*<sup>-/-</sup>*SIX2*<sup>-/-</sup> contains +T of *SIX1* and *SIX2*. **e**, *SIX1*<sup>-/-</sup>*SIX2*<sup>-/-</sup> and *NIK*<sup>-/-</sup> U-2 OS cells are sensitive to BV6/TNF-induced apoptosis. WT, *NIK*<sup>-/-</sup>, or *SIX1*<sup>-/-</sup>*SIX2*<sup>-/-</sup> U-2 OS cells were treated with 25 ng/ml TNF alone or in the presence of indicated concentrations of BV6 for 48 hours. The cell viability was measured by ATP. Cell survival rate was normalized to the absence of BV6 control. **f**, **g**, Expression of cDNAs *SIX2*<sup>R</sup> (see Extended Data Fig. 8e) or *SIX2* protected *SIX1*<sup>-/-</sup>*SIX2*<sup>-/-</sup> or *NIK*<sup>-/-</sup> cells, respectively, from BV6/TNF induced apoptosis. WT, *NIK*<sup>-/-</sup>, or *SIX1*<sup>-/-</sup>*SIX2*<sup>-/-</sup> U-2 OS cells were transduced with *Flu*, *SIX2* or *SIX2*<sup>R</sup> lentivirus as indicated. Cells were then treated with 2.5 μM BV6 plus 25 ng/ml TNF for 24 hours. **h**, **j**, We confirmed that cell death was mediated by the extrinsic apoptotic pathway, as both the pan-Caspase inhibitor (z-VAD) and specific Caspase-8 inhibitor (z-IETD) blocked BV6/TNF-induced cell death *SIX1*<sup>-/-</sup>*SIX2*<sup>-/-</sup> fibroblasts (h) and U-2 OS cells (j). WT and *SIX1*<sup>-/-</sup>*SIX2*<sup>-/-</sup> fibroblasts were treated with 1 μM BV6 plus 10 ng/ml TNF alone or in the presence of 20 μM z-VAD or z-IETD for 24 hours. For U-2 OS experiments, cells were treated with 2.5 μM BV6 plus 25 ng/ml TNF alone or in the presence of 20 μM z-VAD for 48 hours. The cell viability was measured by ATP. Cell survival rate was normalized to each untreated control. **i**, Western blot data showing PARP/Caspase-3 cleavage and the effect of Caspase inhibitors on BV6/TNF

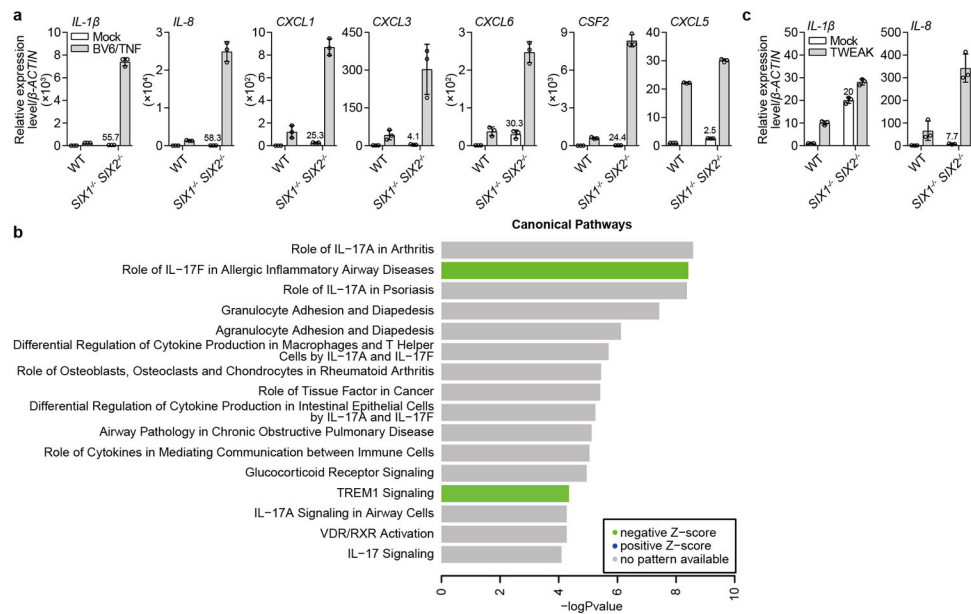
induced cell death of WT and *SIX1*<sup>-/-</sup> *SIX2*<sup>-/-</sup> fibroblasts. Cells were treated with mock, 2.5 μM BV6 plus 25 ng/ml TNF alone or in the presence of 30 μM z-VAD or 40 μM z-IETD for 6 hours. All quantified data are mean±s.d. from 9 (e, f, h, and j) and 6 (g) independent experiments. \**P*<0.05, \*\*\*\**P*<0.0001. Western blot data are representative of 3 independent experiments. For gel source data, see Supplementary Figure 1.

Author Manuscript

Author Manuscript

Author Manuscript

Author Manuscript



### Extended Data Fig. 10. Validation and Pathway analysis of RNA-seq in WT and *SIX1*<sup>-/-</sup> *SIX2*<sup>-/-</sup> H1792 NSCLCs.

**a**, To validate cluster 1 genes from RNA-seq data shown in Fig. 4f, WT and *SIX1*<sup>-/-</sup> *SIX2*<sup>-/-</sup> H1792 cells were treated with mock or 5  $\mu$ M BV6 plus 25 ng/ml TNF for 24 hours. Total RNA was then isolated for qRT-PCR. Gene expression was normalized to WT untreated control. Data are mean $\pm$ s.d. of 3 technical replicates and are representative of 3 independent experiments. **b**, Ingenuity pathway analysis (IPA) of Cluster 1 genes was performed as described in the methods. Pathway enrichment bar plots are shown. Data are from 2 independent experiments. The significance values for the canonical pathways are calculated by Fisher's exact test right tailed. **c**, Experiment showing that inflammatory gene transcription is highly induced in *SIX1*<sup>-/-</sup> *SIX2*<sup>-/-</sup> H1792 cells (compared to WT controls) upon specific stimulation of the non-canonical NF- $\kappa$ B signaling pathway. WT and *SIX1*<sup>-/-</sup> *SIX2*<sup>-/-</sup> H1792 cells were treated with mock or 50 ng/ml TWEAK for 3 hours. Total RNA was extracted for qRT-PCR. Gene expression level was normalized to WT untreated control. Data are mean $\pm$ s.d. of 3 technical replicates and representative of 2 independent experiments.

## ACKNOWLEDGEMENTS

We would like to thank Heide Ford (University of Colorado) for providing the *Tet-on HA-SIX1* transgenic embryos and for helpful discussion in preparation of the manuscript. We also thank UT Southwestern Medical center transgenic core for reviving the frozen embryos, John Minna (UTSW) for providing NSCLCs, and Vincent Tagliabracci, Joshua Mendell, Duoqia Pan, Ivan D'Orso, Nicholas Conrad, and Rolf Brekken and the Alto Lab for helpful discussions. This research was supported by grants from the National Institute of Health (AI083359 to N.M.A and AI117922 to J.W.S.), the Welch Foundation (#I-1731), The Burroughs Welcome Fund, and the Howard Hughes Medical Institute and Simons Foundation Faculty Scholars Program to N.M.A.

## REFERENCES

- Cildir G, Low KC & Tergaonkar V Noncanonical NF-kappaB Signaling in Health and Disease. *Trends Mol Med* 22, 414–429, doi:10.1016/j.molmed.2016.03.002 (2016). [PubMed: 27068135]

2. Sun SC The non-canonical NF-kappaB pathway in immunity and inflammation. *Nat Rev Immunol*, doi:10.1038/nri.2017.52 (2017).
3. Shinkura R et al. Alymphoplasia is caused by a point mutation in the mouse gene encoding Nf-kappa b-inducing kinase. *Nat Genet* 22, 74–77, doi:10.1038/8780 (1999). [PubMed: 10319865]
4. Annunziata CM et al. Frequent engagement of the classical and alternative NF-kappaB pathways by diverse genetic abnormalities in multiple myeloma. *Cancer Cell* 12, 115–130, doi:10.1016/j.ccr.2007.07.004 (2007). [PubMed: 17692804]
5. Keats JJ et al. Promiscuous mutations activate the noncanonical NF-kappaB pathway in multiple myeloma. *Cancer Cell* 12, 131–144, doi:10.1016/j.ccr.2007.07.003 (2007). [PubMed: 17692805]
6. Rosebeck S et al. Cleavage of NIK by the API2-MALT1 fusion oncoprotein leads to noncanonical NF-kappaB activation. *Science* 331, 468–472, doi:10.1126/science.1198946 (2011). [PubMed: 21273489]
7. Xiao G, Harhaj EW & Sun SC NF-kappaB-inducing kinase regulates the processing of NF-kappaB2 p100. *Mol Cell* 7, 401–409 (2001). [PubMed: 11239468]
8. Coope HJ et al. CD40 regulates the processing of NF-kappaB2 p100 to p52. *EMBO J* 21, 5375–5385 (2002). [PubMed: 12374738]
9. Schoggins JW et al. Pan-viral specificity of IFN-induced genes reveals new roles for cGAS in innate immunity. *Nature* 505, 691–695, doi:10.1038/nature12862 (2014). [PubMed: 24284630]
10. Silver SJ & Rebay I Signaling circuitries in development: insights from the retinal determination gene network. *Development* 132, 3–13, doi:10.1242/dev.01539 (2005). [PubMed: 15590745]
11. Ford HL, Kabingu EN, Bump EA, Mutter GL & Pardee AB Abrogation of the G2 cell cycle checkpoint associated with overexpression of HSIX1: a possible mechanism of breast carcinogenesis. *Proc Natl Acad Sci U S A* 95, 12608–12613 (1998). [PubMed: 9770533]
12. Vince JE et al. TWEAK-FN14 signaling induces lysosomal degradation of a cIAP1-TRAF2 complex to sensitize tumor cells to TNFalpha. *J Cell Biol* 182, 171–184, doi:10.1083/jcb.200801010 (2008). [PubMed: 18606850]
13. Varfolomeev E et al. IAP antagonists induce autoubiquitination of c-IAPs, NF-kappaB activation, and TNFalpha-dependent apoptosis. *Cell* 131, 669–681, doi:10.1016/j.cell.2007.10.030 (2007). [PubMed: 18022362]
14. Vince JE et al. IAP antagonists target cIAP1 to induce TNFalpha-dependent apoptosis. *Cell* 131, 682–693, doi:10.1016/j.cell.2007.10.037 (2007). [PubMed: 18022363]
15. Kim JY et al. TNFalpha induced noncanonical NF-kappaB activation is attenuated by RIP1 through stabilization of TRAF2. *J Cell Sci* 124, 647–656, doi:10.1242/jcs.075770 (2011). [PubMed: 21266470]
16. Christensen KL, Brennan JD, Aldridge CS & Ford HL Cell cycle regulation of the human Six1 homeoprotein is mediated by APC(Cdh1). *Oncogene* 26, 3406–3414, doi:10.1038/sj.onc.1210122 (2007). [PubMed: 17130831]
17. Li X et al. Eya protein phosphatase activity regulates Six1-Dach-Eya transcriptional effects in mammalian organogenesis. *Nature* 426, 247–254, doi:10.1038/nature02083 (2003). [PubMed: 14628042]
18. Patrick AN et al. Structure-function analyses of the human SIX1-EYA2 complex reveal insights into metastasis and BOR syndrome. *Nat Struct Mol Biol* 20, 447–453, doi:10.1038/nsmb.2505 (2013). [PubMed: 23435380]
19. Brown K, Gerstberger S, Carlson L, Franzoso G & Siebenlist U Control of I kappa B-alpha proteolysis by site-specific, signal-induced phosphorylation. *Science* 267, 1485–1488 (1995). [PubMed: 7878466]
20. Wertz IE et al. De-ubiquitination and ubiquitin ligase domains of A20 downregulate NF-kappaB signalling. *Nature* 430, 694–699, doi:10.1038/nature02794 (2004). [PubMed: 15258597]
21. Chew J et al. WIP1 phosphatase is a negative regulator of NF-kappaB signalling. *Nat Cell Biol* 11, 659–666, doi:10.1038/ncb1873 (2009). [PubMed: 19377466]
22. Liu B et al. Negative regulation of NF-kappaB signaling by PIAS1. *Mol Cell Biol* 25, 1113–1123, doi:10.1128/MCB.25.3.1113-1123.2005 (2005). [PubMed: 15657437]

23. Sosic D, Richardson JA, Yu K, Ornitz DM & Olson EN Twist regulates cytokine gene expression through a negative feedback loop that represses NF-kappaB activity. *Cell* 112, 169–180 (2003). [PubMed: 12553906]
24. Barboric M, Nissen RM, Kanazawa S, Jabrane-Ferrat N & Peterlin BM NF-kappaB binds P-TEFb to stimulate transcriptional elongation by RNA polymerase II. *Mol Cell* 8, 327–337 (2001). [PubMed: 11545735]
25. McCoy EL et al. Six1 expands the mouse mammary epithelial stem/progenitor cell pool and induces mammary tumors that undergo epithelial-mesenchymal transition. *J Clin Invest* 119, 2663–2677, doi:10.1172/JCI37691 (2009). [PubMed: 19726883]
26. Li L et al. A small molecule Smac mimic potentiates TRAIL- and TNFalpha-mediated cell death. *Science* 305, 1471–1474, doi:10.1126/science.1098231 (2004). [PubMed: 15353805]
27. Petersen SL et al. Autocrine TNFalpha signaling renders human cancer cells susceptible to Smac-mimetic-induced apoptosis. *Cancer Cell* 12, 445–456, doi:10.1016/j.ccr.2007.08.029 (2007). [PubMed: 17996648]
28. Cheung HH et al. SMG1 and NIK regulate apoptosis induced by Smac mimetic compounds. *Cell Death Dis* 2, e146, doi:10.1038/cddis.2011.25 (2011). [PubMed: 21490678]
29. Cheung HH, Mahoney DJ, Lacasse EC & Korneluk RG Down-regulation of c-FLIP Enhances death of cancer cells by smac mimetic compound. *Cancer Res* 69, 7729–7738, doi:10.1158/0008-5472.CAN-09-1794 (2009). [PubMed: 19773432]
30. Fulda S & Vucic D Targeting IAP proteins for therapeutic intervention in cancer. *Nat Rev Drug Discov* 11, 109–124, doi:10.1038/nrd3627 (2012). [PubMed: 22293567]

## METHODS REFERENCES

31. Schoggins JW et al. A diverse range of gene products are effectors of the type I interferon antiviral response. *Nature* 472, 481–485, doi:10.1038/nature09907 (2011). [PubMed: 21478870]
32. Malinin NL, Boldin MP, Kovalenko AV & Wallach D MAP3K-related kinase involved in NF-kappaB induction by TNF, CD95 and IL-1. *Nature* 385, 540–544, doi:10.1038/385540a0 (1997). [PubMed: 9020361]
33. Yin L et al. Defective lymphotoxin-beta receptor-induced NF-kappaB transcriptional activity in NIK-deficient mice. *Science* 291, 2162–2165, doi:10.1126/science.1058453 (2001). [PubMed: 11251123]
34. Zhang X, Goncalves R & Mosser DM The isolation and characterization of murine macrophages. *Curr Protoc Immunol* Chapter 14, Unit 14 11, doi:10.1002/0471142735.im1401s83 (2008).
35. Sanjana NE, Shalem O & Zhang F Improved vectors and genome-wide libraries for CRISPR screening. *Nat Methods* 11, 783–784, doi:10.1038/nmeth.3047 (2014). [PubMed: 25075903]
36. Tetsuka T et al. Inhibition of nuclear factor-kappaB-mediated transcription by association with the amino-terminal enhancer of split, a Groucho-related protein lacking WD40 repeats. *J Biol Chem* 275, 4383–4390 (2000). [PubMed: 10660609]
37. Perelman SS et al. Cell-Based Screen Identifies Human Interferon-Stimulated Regulators of *Listeria monocytogenes* Infection. *PLoS Pathog* 12, e1006102, doi:10.1371/journal.ppat.1006102 (2016). [PubMed: 28002492]
38. Trapnell C et al. Differential gene and transcript expression analysis of RNA-seq experiments with TopHat and Cufflinks. *Nat Protoc* 7, 562–578, doi:10.1038/nprot.2012.016 (2012). [PubMed: 22383036]
39. Aronesty E Comparison of sequencing utility programs. *Open Bioinformatics J* 7, 1–8, doi:10.2174/1875036201307010001 (2013).
40. Kim D et al. TopHat2: accurate alignment of transcriptomes in the presence of insertions, deletions and gene fusions. *Genome Biol* 14, R36, doi:10.1186/gb-2013-14-4-r36 (2013). [PubMed: 23618408]
41. Liao Y, Smyth GK & Shi W featureCounts: an efficient general purpose program for assigning sequence reads to genomic features. *Bioinformatics* 30, 923–930, doi:10.1093/bioinformatics/btt656 (2014). [PubMed: 24227677]

42. Robinson MD, McCarthy DJ & Smyth GK edgeR: a Bioconductor package for differential expression analysis of digital gene expression data. *Bioinformatics* 26, 139–140, doi:10.1093/bioinformatics/btp616 (2010). [PubMed: 19910308]
43. Cormier CY et al. Protein Structure Initiative Material Repository: an open shared public resource of structural genomics plasmids for the biological community. *Nucleic Acids Res* 38, D743–749, doi:10.1093/nar/gkp999 (2010). [PubMed: 19906724]
44. Dittmann M et al. A serpin shapes the extracellular environment to prevent influenza A virus maturation. *Cell* 160, 631–643, doi:10.1016/j.cell.2015.01.040 (2015). [PubMed: 25679759]
45. Bhattacharyya S, Borthakur A, Dudeja PK & Tobacman JK Lipopolysaccharide-induced activation of NF-kappaB non-canonical pathway requires BCL10 serine 138 and NIK phosphorylations. *Exp Cell Res* 316, 3317–3327, doi:10.1016/j.yexcr.2010.05.004 (2010). [PubMed: 20466000]
46. Kumar JP The sine oculis homeobox (SIX) family of transcription factors as regulators of development and disease. *Cell Mol Life Sci* 66, 565–583, doi:10.1007/s00018-008-8335-4 (2009). [PubMed: 18989625]

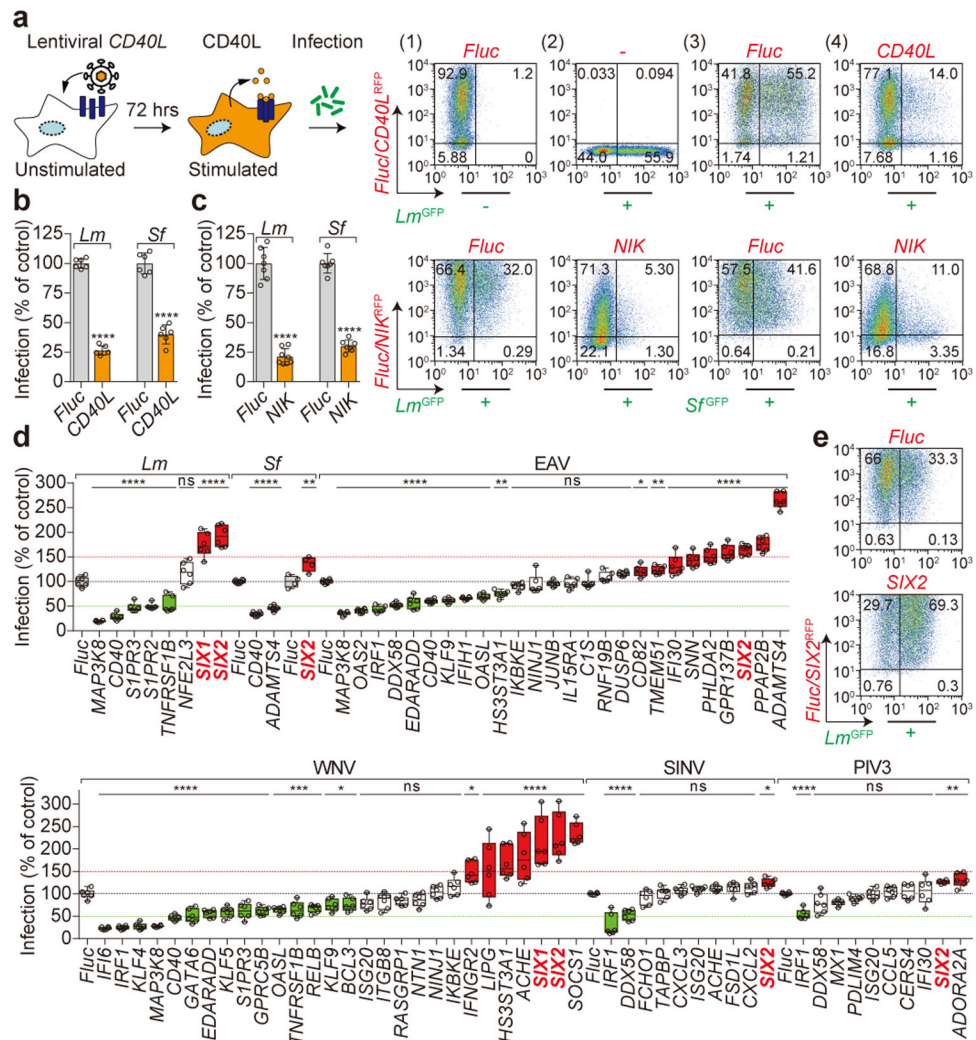


**Figure 1. SIX-proteins exhibit immunomodulatory functions.**

**a, b,** Diagram and data showing lentiviral delivery of *CD40L*/RFP into U-2 OS cells and its effect on GFP-expressing *Lm* infection. Representative flow cytometry scatter plots showing (1) *luciferase* (*Fluc*)<sup>RFP</sup> transduced uninfected cells, (2) untransduced *Lm*<sup>GFP</sup> infected cells, (3) *Fluc*<sup>RFP</sup> transduced cells infected with *Lm*<sup>GFP</sup>, and (4) *CD40L*<sup>RFP</sup> transduced cells infected with *Lm*<sup>GFP</sup> (a). Quantification of *Lm* and *Sf* infection of *CD40L* transduced cells as indicated (b). Bacterial infectivity was normalized to *Fluc* control (shown as 100%). Data are mean±s.d. from 6 independent experiments, \*\*\*\*  $P < 0.0001$ ,  $P$  values were derived from biological replicates using one-way ANOVA (GraphPad). The same statistics were applied to later studies unless otherwise stated. **c,** Fibroblasts transduced with *Fluc* or *NIK* lentivirus and then infected with GFP expressing *Lm* and *Sf* as indicated. Quantification of infection is presented as in b. Data are mean±s.d. from 6 independent experiments, \*\*\*\*  $P < 0.0001$ . Representative flow cytometry scatter plots showing infection efficiency as described in a. **d,** Repeated trials of *NIK*-stimulated genes that inhibit (green) or enhance (red) infection by bacterial pathogens (*Lm* and *Sf*), +ssRNA viral pathogens (EAV: equine arteritis virus, WNV: West Nile virus, and SINV: Sindbis virus), and +ssRNA viral pathogen (PIV3: parainfluenza virus type 3). The relative percentage of pathogen infection was normalized to

*Fluc* control (black dotted line). Data are presented as box and whisker plots, box is percentiles, black line is the population median, whiskers indicating the highest and lowest values (6 independent experiments). \* $P < 0.05$ , \*\* $P < 0.01$ , \*\*\* $P < 0.001$ , \*\*\*\* $P < 0.0001$ , ns: no significant difference. **e.** Representative flow cytometry scatter plots showing *Lm* infection efficiency in *Fluc* and *SIX2* expressed fibroblasts as described in a. Data are representative of 6 independent experiments.

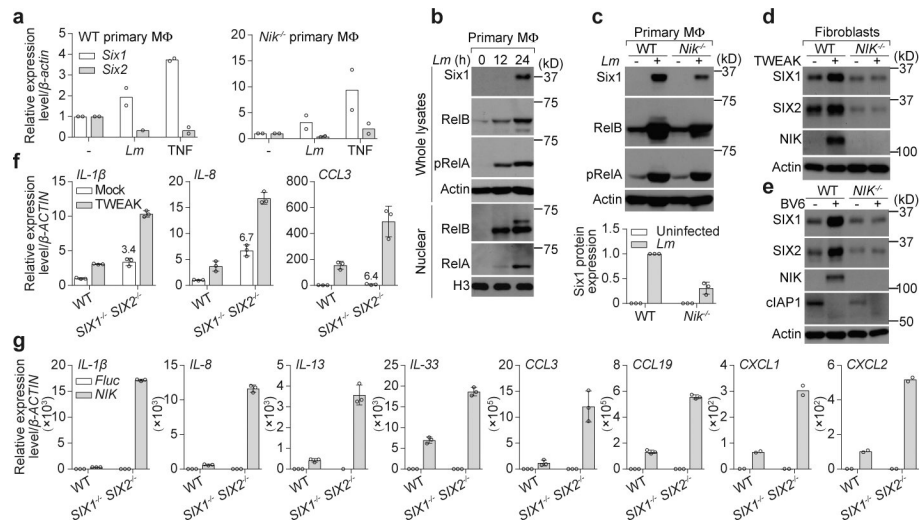


**Figure 2. Reactivation of SIX1 and SIX2 by NIK results in inflammatory gene suppression.**  
**a**, qRT-PCR of total RNA isolated from WT or *Nik*<sup>-/-</sup> primary BMDMs infected with *Lm* (MOI=0.1) or treated with 25 ng/ml TNF for 24 hours. The relative gene expression was normalized to untreated control. Bars are the mean from 2 independent experiments and circles are the average of 2 technical replicates from each experiment. **b**, **c**, Levels of Six1 protein in WT or *Nik*<sup>-/-</sup> primary BMDMs infected with *Lm* (MOI~0.1) for indicated time points (**b**) or for 24 hours (**c**). Whole cell lysate or nuclear extracts were probed with indicated antibodies by western blot. Quantification of Six1 protein levels (mean±s.d. from 3 independent experiments) in the indicated samples were normalized to WT cells (1.0). **d**, **e**, SIX1 expression levels in WT and *NIK*<sup>-/-</sup> fibroblasts treated with 50 ng/ml TWEAK (**d**) or 5 μM BV6 (**e**) for 24 hours and processed for western blot analysis as in **b**. **f**, qRT-PCR of total RNA isolated from WT and *SIX1*<sup>-/-</sup> *SIX2*<sup>-/-</sup> fibroblasts treated with 50 ng/ml TWEAK for 24 hours. The relative gene expression was normalized to WT untreated control and shown as mean±s.d. of 3 technical replicates from one experiment. Data are representative of 3 independent experiments. **g**, qRT-PCR of total RNA isolated from WT and *SIX1*<sup>-/-</sup> *SIX2*<sup>-/-</sup> fibroblasts transduced with *Fluc* or *NIK* lentivirus for 72 hours. The relative gene expression was normalized to WT *Fluc* transduced control and shown as mean ±s.d. of 3 technical replicates from one experiment. Data are representative of 3 independent experiments. All western blot data are representative of 3 independent experiments. For gel source data, see Supplementary Figure 1.

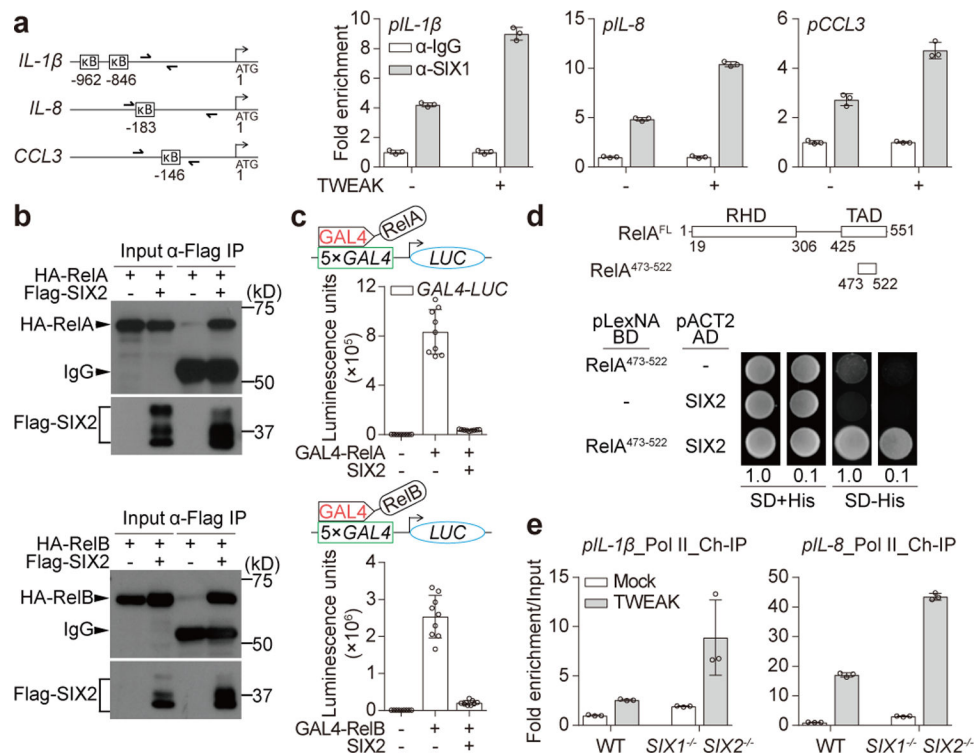


**Figure 3. SIX-family transcription factors directly inhibit promoter bound NF- $\kappa$ B.**

**a**, ChIP qPCR analysis of SIX1 occupancy of the indicated genes from fibroblasts treated with mock or 50 ng/ml TWEAK for 2 hours. Location of each primer set compared to the gene start sites (ATG) and  $\kappa$ B sites are shown (diagram). IgG control samples were normalized to 1.0 and relative fold enrichment of SIX1 is shown as mean $\pm$ s.d. of 3 technical replicates from one experiment. Data are representative of 3 independent experiments. **b**, Western blot showing input and Co-Immunoprecipitation (Co-IP) of Flag-SIX2 and association with HA-RelA (upper blot) or HA-RelB (lower blot) expressed in HEK293T cells. **c**, Graph showing luminescence units from 5 $\times$ GAL4-Luciferase reporter gene driven by RelA (upper) and RelB (lower) fused to GAL4 DNA-binding domain. Reporter constructs were co-transfected with or without SIX2 and measured after 48 hours as indicated. Data are mean $\pm$ s.d. from 9 independent experiments. **d**, Yeast two hybrid analysis of SIX2 binding to RelA TAD domain. Diagram shows RelA domains (RHD: Rel homology domain, TAD: Transactivation domain). Yeast transformed with the indicated plasmids were serially diluted and spotted on SD/UWL<sup>-</sup> (SD+His) or SD/WHULK<sup>-</sup> (SD-His) used to detect His-reporter gene activation by protein-protein interactions (bottom). **e**, The relative fold enrichment of RNA Pol II on the indicated genes in mock or 50 ng/ml TWEAK (2 hours) treatment of WT or  $SIX1^{-/-}$   $SIX2^{-/-}$  fibroblasts as in **a**. Mock treated WT fibroblasts were normalized to 1.0 by adjusting to “input DNA” that was saved prior to immunoprecipitation. Relative fold enrichment of RNA Pol II is shown as mean $\pm$ s.d. of 3 technical replicates from one experiment. Data are representative of 3 independent experiments. All western blot and yeast two hybrid data are representative of 3 independent experiments. For gel source data, see Supplementary Figure 1.

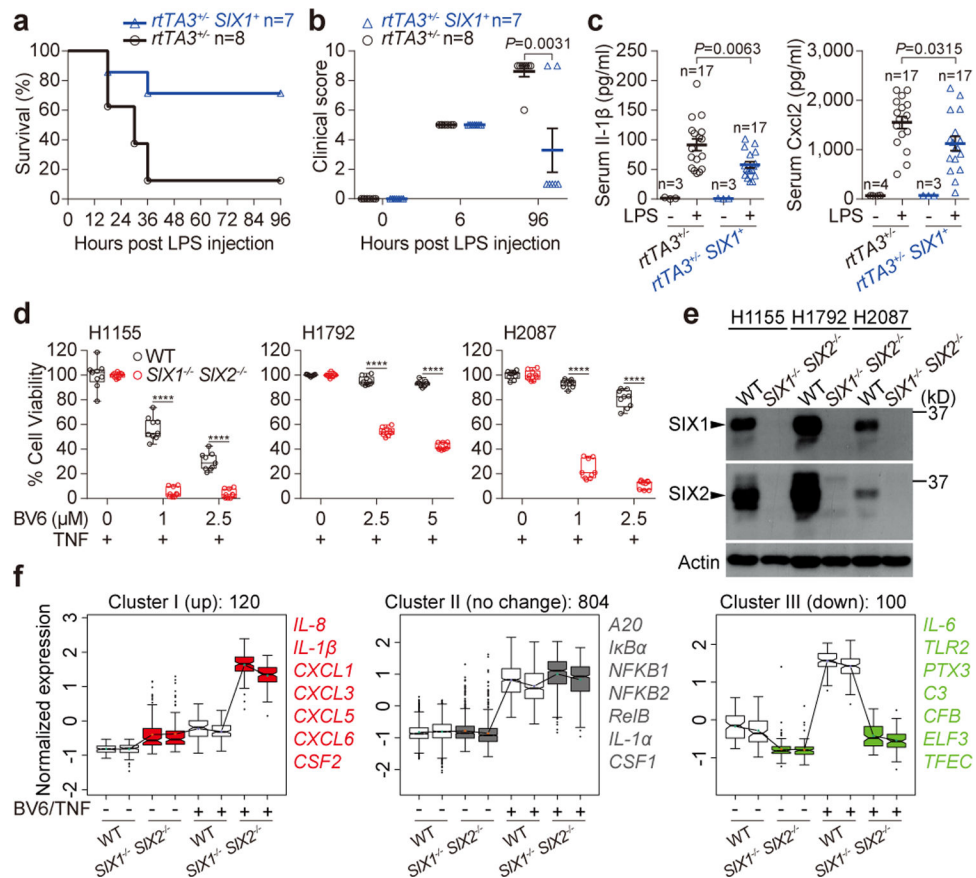


**Figure 4. Physiological and pathological roles of the NIK-SIX signaling axis.**

**a, b,** *rtTA3<sup>+/+</sup> SIX1<sup>+</sup>* mice or littermate controls (*rtTA3<sup>+/+</sup>*) were challenged with LPS as described in Extended Data Fig. 7f. LPS-induced survival curve (a) and clinical score outcome (b) are representative of 3 independent experiments. The number of animals (n) are shown. Data are mean±s.e.m and *P* value was measured by two tailed unpaired Student's *t*-test (b). **c,** serum IL-1 $\beta$  and Cxcl2 production in the indicated genotypes treated with LPS as described in Extended Data Fig. 7f. The number of animals (n) are shown. *P* value was measured by two tailed unpaired Student's *t*-test. **d, e,** H1155 (left), H1792 (middle), or H2087 (right) cells were treated with 10 ng/ml TNF alone or in the presence of BV6 for 24 hours. Cell survival rate was normalized to the absence of BV6 control. Data are presented as box and whisker plots (9 independent experiments). Box is percentiles, line is the population median, and whiskers indicate the highest and lowest values. \*\*\*\**P*<0.0001 (d). Western blot showing endogenous SIX1 and SIX2 expression in the indicated cells (e). Data are representative of 3 independent experiments. **f,** RNA-seq data from WT and *SIX1<sup>-/-</sup> SIX2<sup>-/-</sup>* H1792 cells treated with mock or 5  $\mu$ M BV6 plus 25 ng/ml TNF for 24 hours. 1024 genes were significantly induced by BV6/TNF treatment in WT cells (statistical test is presented in methods). 120 out of 1024 genes were significantly upregulated (left), 804 genes were unchanged (middle), and 100 genes were downregulated (right) in *SIX1<sup>-/-</sup> SIX2<sup>-/-</sup>* cells. The representative genes were listed. Data are from 2 independent experiments and presented as box and whisker plots. Box is percentiles and line is the

population median from the indicated number of genes. For gel source data, see Supplementary Figure 1.

Author Manuscript

Author Manuscript

Author Manuscript

Author Manuscript